



Minerva Access is the Institutional Repository of The University of Melbourne

Author/s:

Sarhan, AAR;Franklyn, M;Lee, PVS

Title:

The use of finite element models for backface deformation and body armour design: a systematic review

Date:

2025-01-01

Citation:

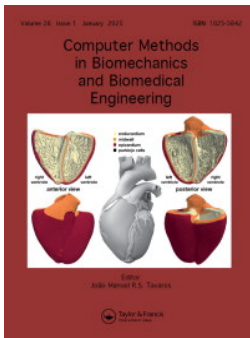
Sarhan, A. A. R., Franklyn, M. & Lee, P. V. S. (2025). The use of finite element models for backface deformation and body armour design: a systematic review. *Computer Methods in Biomechanics and Biomedical Engineering*, 28 (1), pp.121-143. <https://doi.org/10.1080/10255842.2023.2281275>.

Persistent Link:

<https://hdl.handle.net/11343/363443>

License:

[CC BY-NC-ND](#)



# Computer Methods in Biomechanics and Biomedical Engineering

ISSN: 1025-5842 (Print) 1476-8259 (Online) Journal homepage: [www.tandfonline.com/journals/gcmb20](http://www.tandfonline.com/journals/gcmb20)

## The use of finite element models for backface deformation and body armour design: a systematic review

Abd Alhamid R. Sarhan, Melanie Franklyn & Peter V. S. Lee

To cite this article: Abd Alhamid R. Sarhan, Melanie Franklyn & Peter V. S. Lee (2025) The use of finite element models for backface deformation and body armour design: a systematic review, *Computer Methods in Biomechanics and Biomedical Engineering*, 28:1, 121-143, DOI: [10.1080/10255842.2023.2281275](https://doi.org/10.1080/10255842.2023.2281275)

To link to this article: <https://doi.org/10.1080/10255842.2023.2281275>



© 2023 The Author(s). Published by Informa UK Limited, trading as Taylor & Francis Group



Published online: 14 Nov 2023.



Submit your article to this journal [↗](#)



Article views: 2098



View related articles [↗](#)



View Crossmark data [↗](#)

# The use of finite element models for backface deformation and body armour design: a systematic review

Abd Alhamid R. Sarhan<sup>a</sup>, Melanie Franklyn<sup>b</sup> and Peter V. S. Lee<sup>a</sup>

<sup>a</sup>Department of Biomedical Engineering, University of Melbourne, Melbourne, VIC, Australia; <sup>b</sup>Defence Science and Technology Group (DSTG), Melbourne, VIC, Australia

## ABSTRACT

While injuries sustained from body armour backface deformation (BFD) have not been well-documented in military injury trauma registries, data from US law enforcement officers, animal tests and currently available data pertaining to military combatants has shown that BFD can not only cause minor injuries, but also result in serious trauma. However, the nature and severity of injuries sustained depends on a multitude of factors including the projectile type, the impact location and velocity, and the specific type of body armour worn. The difficulties involved in current measurement techniques for ballistic testing has led researchers to seek alternative techniques to evaluate the level of protection from body armour, such as the finite element (FE) method. In the current study, a systematic review of the open literature was undertaken using the Preferred Reporting Items for Systematic Reviews and Meta-Analyses methodology. The aim was to summarise the literature pertaining to the development and application of FE models to investigate body armour BFD and behind armour blunt trauma (BABT), and included FE models representing the projectile, clay-based mediums, ballistic gelatine and the human torso. Using the keywords 'behind armour\*', 'ballistic blunt trauma', 'BABT', 'backface signature', 'backface deformation', 'BFS', 'BFD', 'wound ballistic', 'ballistic impact testing', 'body armour', 'bullet proof vest', 'ballistic vest', 'Finite Element\*' and 'FE', an electronic database search of EBSCOhost, Google Scholar, ProQuest, Scopus, Standards, Web of Science and PubMed was conducted, and included peer-reviewed journal articles, review papers, research reports, conference papers, and MSc or PhD theses. While this research demonstrates the potential of FE analysis for recreating realistic blunt impact scenarios and enhancing the current understanding of BABT mechanisms, a common limitation in most studies is the lack of validation. Thus, in order to address this issue, it is proposed that injury predictions from FE models be correlated with trauma data from soldiers who have sustained BABT. Consequently, pressure and energy distributions within the organs can be used to interpret the effects of non-penetrating ballistic impacts on the human torso. Bridging the gap between simulation and real-world data is essential in order to validate FE models and enhance their utility in optimising body armour design and employing injury mitigation strategies.

## ARTICLE HISTORY

Received 28 July 2023  
Accepted 3 November 2023

## KEYWORDS

Systematic review; finite element modelling; ballistic blunt impact; backface deformation; behind-armour blunt trauma

## 1. Introduction

Body armour is employed in both civilian and military scenarios to prevent penetrating injuries from high-velocity projectiles. A critical aspect of body armour performance is its ability to withstand non-penetrating ballistic impacts, which can result in rapid displacement and deformation of the armour. This displacement generates a significant amount of energy that dissipates and propagates throughout the plate and underlying tissues, including energy transmission to organs not directly underneath the body armour (Lim, Shim, and Ng 2003; Dominiak and Stempień

2012; Graham and Zhang 2019). The injuries sustained from the underlying blunt impact are known as behind armour blunt trauma (BABT) (Lewis 2005; Gilson et al. 2020), and may include skin contusions and penetrations (Chang 2001); rib fractures (Niu, Shen, and Stuhmiller 2007); sternal fractures (Talmy et al. 2023); and contusions to internal organs such as the lungs, kidneys, and spleen, and in rare cases, the heart (Rocksén et al. 2020; Eaton, McMahon, and Salzar 2022). At the impact location, the velocity of the armour deformation and the wall of the thorax rapidly increase to reach maximum values within a few hundred microseconds. This is followed by an

**CONTACT** Abd Alhamid R. Sarhan  [hamid.sarhan@unimelb.edu.au](mailto:hamid.sarhan@unimelb.edu.au)

© 2023 The Author(s). Published by Informa UK Limited, trading as Taylor & Francis Group  
This is an Open Access article distributed under the terms of the Creative Commons Attribution-NonCommercial-NoDerivatives License (<http://creativecommons.org/licenses/by-nc-nd/4.0/>), which permits non-commercial re-use, distribution, and reproduction in any medium, provided the original work is properly cited, and is not altered, transformed, or built upon in any way. The terms on which this article has been published allow the posting of the Accepted Manuscript in a repository by the author(s) or with their consent.

exponential decrease in velocity until the maximum BFD is achieved within a few milliseconds (Cronin 2012). The shear stresses generated from the impact can result in tearing of tissues due to the inability of organs to withstand the high rate of loading from the impact event (Seng et al. 2021).

The nature, severity, and extent of injuries resulting from BFD depend upon a multitude of factors, including the type and thickness of the body armour, the material layout, and factors relating to the impact itself such as the impact velocity, calibre of the projectile, and the angle at which the projectile strikes the body armour (Tam, Dorn, and Gotts 2000). Despite there being no documented evidence for fatalities due to BFD in either military or civilian contexts (Carr, Horsfall, and Malbon 2016), data from US law enforcement officers, animal tests and military combatant in-theatre data (i.e. data from areas of significant military events or operations) has shown that BFD can potentially result in injuries ranging from minor to serious trauma (Mauzac et al. 2012). For example, an analysis of 90 shots defeated by body armour to 71 US law enforcement officers demonstrated that the injuries ranged from minor (soft tissue wounds) to more severe trauma such as rib fractures, liver lacerations and lung contusions (Bir 2000). Moreover, as body armour design continues to be developed and optimised, resulting in thinner, lighter, and more deformable armours, an increased risk from BFD may emerge (Bouamoul and Lévesque 2007).

Over the past few decades, there has been an increasing interest in developing new experimental techniques to assess body armour (Liden et al. 1988; Cronin et al. 2001). In 1970s, the National Institute of Justice (NIJ) adopted the most widely referenced ballistic standard, NIJ 44 mm BFD standard, which specifies the amount of BFD allowed in protective materials for five different types of protection classifications (II-IV) (Merkle et al. 2008). The specification states that the residual BFD depth or backface signature (BFS) in a clay medium cannot be greater than 44 mm when a series of standard impacts on an armour plate strapped over Roma Plastilina No. 1 clay (RP1 clay), mounted in a rigid box, are performed (Rahbek 2015). However, while the efficiency of body armour continues to be tested using the NIJ's clay standard, it is widely acknowledged that the 44 mm maximum assessment is, at best, inadequate, having never been correlated with human injuries. Furthermore, with only a pass/fail result, the standard provides no means for the design, assessment, and optimisation of body armour. It also is unknown how

a maximal depth of 44 mm BFD into clay was initially translated into a torso response (Kim et al. 2022a). Moreover, the standard does not factor parameters such as BFD volume and area, the rate of body wall deflection, or the position of the impact on the plate, all of which are significant characteristics dictating the types of injuries sustained and overall level of trauma (Cannon 2001; Bass et al. 2006). A further limitation is that the NIJ's clay standard was based on the compliance of soft tissues in the abdomen, whereas impacts to the thorax would respond differently because there is less soft-tissue coverage over the thorax than the abdomen, and thus the injury thresholds between the two body regions are likely to differ (Rahman 2013; Bustamante et al. 2019). Consequently, body armour may be overengineered, being heavier than required, leading to a weight burden on the soldiers and a negative impact on mobility, manoeuvrability and performance. Lastly, the response of the backing material used in testing, RP1 clay, significantly differs from the behaviour of human tissues under ballistic impact (Bracq et al. 2019; Zochowski 2019; Batra and Pydah 2020; Bracq 2021).

The limitations inherent in the current ballistic clay-based standard have led researchers to explore alternative methods of assessment such as the FE (finite element) method, an advanced computational technique used in a range of applications to solve numerical problems in fields such as aerospace, automotive and civil engineering as well as impact biomechanics in order to simulate the behaviour of complex structures and materials under various impact conditions. In the context of body armour research, FE analysis can be an invaluable tool for modelling and analysing the response of armour materials, human tissues, and other relevant components when they subjected to ballistic and blunt impacts, including the effects of BFD.

Due to the continual increase in computational power over the last few decades, the FE method has become one of the most commonly used mathematical approaches employed for understanding body armour BFD and the mechanical response of the human torso under ballistic impacts. In this context, FE analysis has numerous advantages over experimental testing, including the capability to perform a large number of simulations in a relatively short time period, and the ability to obtain a better understanding of the mechanisms occurring during the BFD event (Hampton and Kleinberger 2018a). Advanced FE codes such as LS-DYNA, RADIOSS, NASTRAN, and ABAQUS have been widely used by researchers to simulate ballistic impacts on the human body, as

these sophisticated FE programs have the capability to handle complex material compositions, boundary conditions, and non-linearity. Of these programs, LS-DYNA has been most extensively used, most likely because of the large library of material models available: LS-DYNA includes more than a hundred of material constitutive models and ten equations-of-state (EoS) which cover a wide range of material behaviour, from elastic to elastic-plastic and strain-rate-dependent materials. LS-DYNA also contains various contact-impact algorithms, such as surface-to-surface, node-to-surface, node-tied-to-surface, and surface-tied-to-surface, which allow difficult contact problems to be solved more readily (Rahman 2013).

While a number of studies over the past two decades have contributed to better understanding the relationship between BFD and the mechanical response of the human torso, body armour materials and design continue to develop and evolve, resulting in lighter weight and more deformable plates, potentially increasing the risk and severity of injuries from BFD. Thus, it is critical to ascertain the protective capabilities of new novel material layouts and armour designs, and more specifically, the level of trauma they can mitigate. However, the tenuous relationship of the current BFD standard with injury combined with its other limiting factors limits its relevance and use in ballistic testing, body armour design and plate optimisation. Consequently, there is a need to establish the status of current research pertaining to the application of advanced computational models in BFD and body armour design. Thus, in the current study, the pertinent characteristics of FE models used for ballistic simulations have been systematically reviewed, including numerical models representing: 1. projectiles; 2. clay and gelatine testing blocks and 3. the human torso. To ensure a precise understanding of the terminology employed throughout this study, the following explicit definitions have been used: 'ballistic impact' refers to high-velocity collisions typically associated with projectiles, such as bullets or shrapnel. These impacts involve rapid motion and are characterized by their potential to penetrate or perforate materials. On the other hand, 'blunt impact' refers to collisions or impacts involving objects or forces distributed over a broader surface area, rather than being sharp or pointed. Blunt impacts are often associated with injuries caused by forces applied over a larger region.

## 2. Methodology

In the current study, a systematic review was conducted in line with the Preferred Reporting Items for

Systematic Reviews and Meta-Analyses (PRISMA) guidelines and methodology (Liberati et al. 2009; Scherer and Saldanha 2019; Page et al. 2021). The open literature was searched for published papers in English pertaining to the development or application of FE models to investigate torso BFD. The review included articles published between 1<sup>st</sup> January 1980 and 1<sup>st</sup> December 2022 where the following electronic databases were queried: EBSCOhost, Google Scholar, ProQuest, Scopus, Standards, Web of Science, and PubMed. This search encompassed peer-reviewed journal articles, review papers, research reports, conference papers, MSc theses, and PhD theses. The keywords applied were 'behind armour\*', 'ballistic blunt trauma', 'BABT', 'backface signature', 'backface deformation', 'BFS', 'BFD', 'wound ballistic', 'Ballistic impact testing', 'body armour', 'bullet proof vest', 'ballistic vest', 'Finite Element\*' and 'FE'. The title, abstract, keywords, journal name, and year of publication of the relevant papers were exported to an excel spreadsheet before initial screening of the titles and abstracts was performed by the authors. The full texts of the remaining papers were subsequently assessed based on the eligibility criteria, which were: (1) finite element models; (2) thorax region only; (3) investigated behind armour blunt trauma from ballistic impacts; (4) addressed the relationship between BFD and BABT and (5) written in English. The exclusion criteria were: (1) experimental studies; (2) research using analytical and statistical methods; (3) FE models used to study blunt trauma in automotive crashes and (4) published before 1980 (since FE models prior to that time were predominately preliminary or basic FE models). The reference section from any included studies was also searched in order to identify additional relevant papers which may have been missed.

## 3. Results

Although the search of the electronic databases retrieved 789 records, 338 publications were excluded due to duplications. To ensure the quality and relevance of the academic literature included in this review, the abstracts of the remaining records were subsequently checked in greater detail. Three hundred seventy-six of these publications were discarded because they did not meet the eligibility criteria. A further review of the 75 remaining papers revealed that three papers were not in English, consequently they were discarded, leaving 72 papers remaining. References from the included studies, which had also been checked, revealed no additional publications

meeting the inclusion criteria which had not already been identified in electronic search, thus there was a total of 72 papers for the systematic review. A flow-chart of the selection process is depicted in Figure 1.

Thus, the following sections outline studies where the FE method has been employed to simulate the mechanical responses from ballistic impacts to clay, gelatine, and the torso, where computational models are presented of the 3.1: Projectile; 3.2 Clay block; 3.3. Gelatine block and 3.4 Human Torso. Clay (RP1 clay) and gelatine (a mixture of 10% or 20% gelatine powder and water) were included as these backing materials have frequently been used as human body surrogates in ballistic testing.

### 3.1. Finite element models of projectiles

Table 1 provides a comprehensive overview of various projectile models which have been used in the literature, specifically focusing on their geometries, masses, impact velocities, and the associated material models employed to simulate them. These projectile models have been used to either simulate an impact to the body armour directly, or to simulate a blunt impactor

directly striking the torso, clay or gelatine in order to replicate armour BFD. This data can be of aid to researchers simulating ballistic impacts, providing crucial information on relevant parameters and characteristics of the projectiles commonly used in this context.

Obtaining the geometry for a specific projectile is relatively straightforward, however, as projectiles are manufactured using a range of materials which differ in their dynamic behaviour under impact, accurate material characterisation is critical to simulate the deformation of the projectile during the impact event. The material model employed depends on both the projectile type and the application. For example, it is common to treat a steel sphere as rigid object in order to reduce computational expense (Gad and Gao 2020; Ye et al. 2022), which is a reasonable assumption as the stiffness of a steel sphere is several orders of magnitude greater than that of RP1 clay (Gad and Gao 2020). However, static material characteristics are often not sufficient to obtain valid results because the loading rates in a ballistic event are outside the range of quasi-static tests. Consequently, employing constitutive models that can account for the dynamic

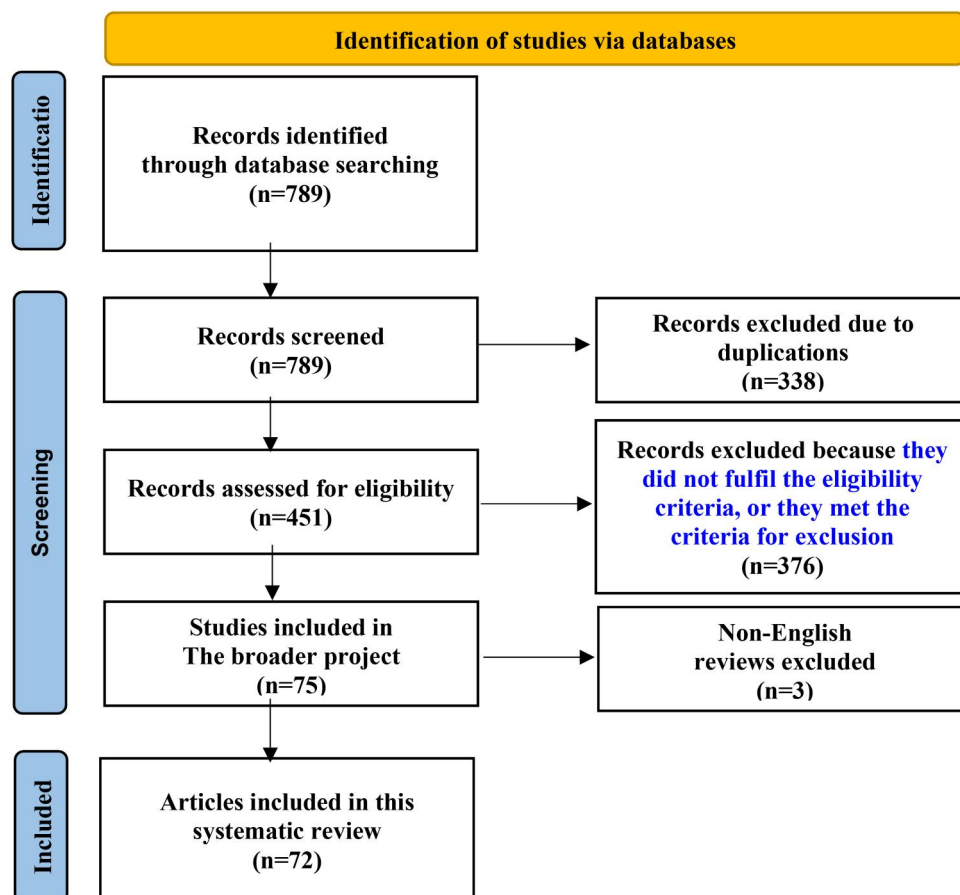


Figure 1. Flowchart of the study selection process.

**Table 1.** A summary of physical and geometrical properties of projectiles which have previously been modelled using FE analysis.

Projectile Size	Projectile Type	Refs	Mass	Velocity	Material Model Name	Material Model Properties	Impact Type <sup>#</sup>
$D = 9\text{ mm}$	Luger	Zochowski (2019)	7.45 g	50 – 150 m/sec	*MAT_107	<ul style="list-style-type: none"> <li>• Adiabatic heating included in the material formulation.</li> <li>• Model cannot be used in mechanical analysis where temperature is prescribed using *LOAD_THERMAL</li> </ul>	Ballistic
	FMJ	Shen et al. (2010)	8.04 g	452 m/sec	*MAT_003	<ul style="list-style-type: none"> <li>• This model is suited for modelling isotropic and kinematic hardening plasticity.</li> <li>• Very cost effective model</li> </ul>	Ballistic
	Bullet	Roberts, O'Connor, and Ward (2005)	8 g	360 – 425 m/sec	*MAT_003	<ul style="list-style-type: none"> <li>• Model is suited for modelling isotropic and kinematic hardening plasticity.</li> <li>• Very cost effective model</li> </ul>	Ballistic
$D = 7.62\text{ mm}$	PS	Zochowski (2019)	7.9 g	50 – 150 m/sec	*MAT_107	<ul style="list-style-type: none"> <li>• Adiabatic heating was included in the material formulation.</li> <li>• Model cannot be used in mechanical analysis where temperature is prescribed using *LOAD_THERMAL.</li> </ul>	Ballistic
$D = 12.7\text{ mm}$	FSP	Chan (2021)	13.14 g	300–600 m/s	*MAT_020	<ul style="list-style-type: none"> <li>• Optional global and local constraints on the mass centre can be defined</li> </ul>	Ballistic
$D = 20\text{ mm}$		Nguyen et al. (2016)	53.7 g	365, 615, 911, 1410 and 1966 m/s	*MAT_015	<ul style="list-style-type: none"> <li>• Model requires the use of the shock formulation of the Mie-Grüneisen EoS</li> </ul>	Ballistic
$D = 37\text{ mm}$ $L = 100\text{ mm}$	PVC	Ndompetelo (2016)	140 g	20, 40, 60 m/sec	*MAT_001	<ul style="list-style-type: none"> <li>• Isotropic elastic material</li> </ul>	Blunt BFD
$D = 20\text{ mm}$	Cylindrical silicone	Ng and Niu (2018)	50 g	40 m/sec	*MAT_007	<ul style="list-style-type: none"> <li>• The simplified model can be used with beam elements.</li> </ul>	Blunt BFD
$D = 152.4\text{ mm}$	Cylindrical steel	Hampton and Kleinberger (2018b)	22.9 – 23.6 kg	6.7 – 7.4 m/sec	*MAT_001	<ul style="list-style-type: none"> <li>• Isotropic elastic material</li> </ul>	Blunt BFD

D = Diameter of projectile; L = Length of the projectile.

FMJ: Full Metal Jacket.

PS: Púlya so Stal'ným serdéchnikom - Bullet with a Steel core.

FSP: Fragment Simulating Projectile.

PVC: Polyvinyl Chloride.

Ballistic impact: A ballistic projectile impacting body armour directly; Blunt BFD: Blunt impactor directly striking the torso, or clay, or gelatine to simulate armour BFD.

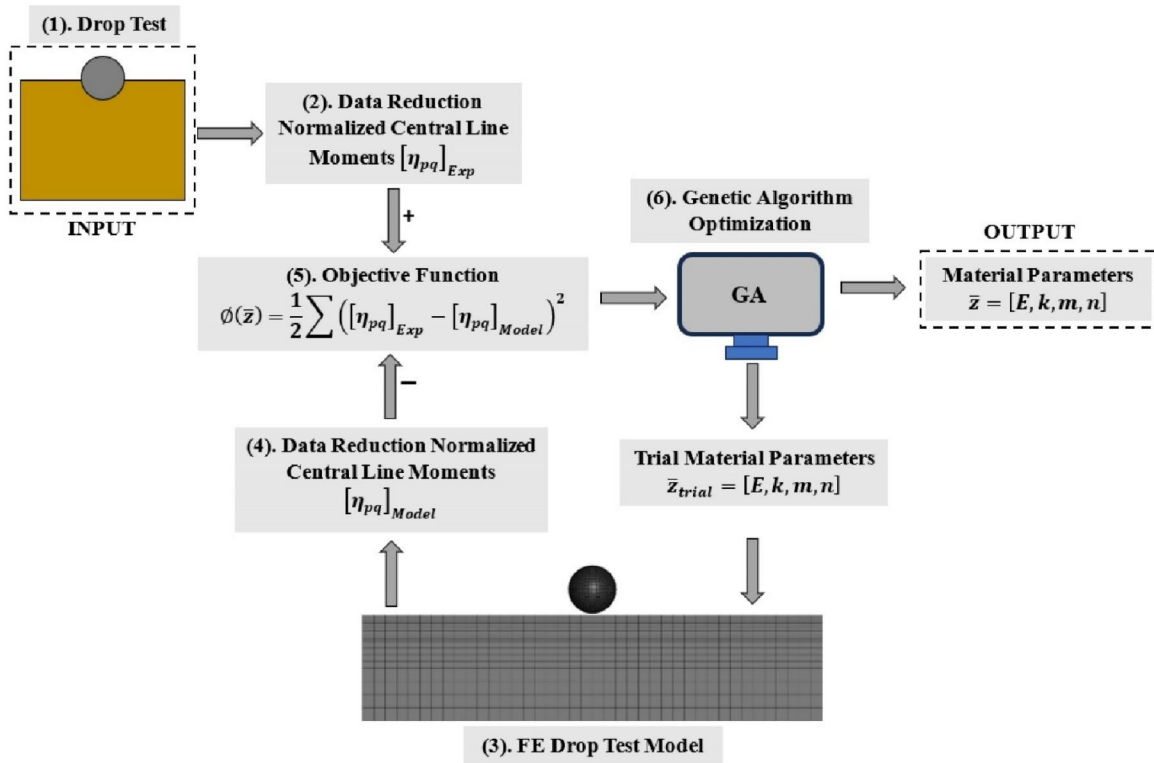
behaviour of the projectile improves the material response under operational loading conditions, particularly at high velocities (Breeze et al. 2014; Ndompetelo 2016).

### 3.2. Finite element models of the clay block

RP1 clay is a homogeneous malleable synthetic clay, made from oils, waxes and minerals. Although it was originally used for artistic applications, for example, as a modelling clay for making sculptures, its soft plastic nature has led to its use in certain engineering applications such as metal forming analysis. RP1 clay is currently widely employed as backing material to replicate the human torso tissue in ballistic resistance testing of body armours, where it is used to evaluate the potential trauma sustained from a non-penetrating ballistic impact (Hernandez, Buchely, and Maranon 2015). Thus,

ascertaining the characteristics and behaviour of this material is critical in order to understand body armour ballistic performance.

Unlike traditional clay, RP1 clay contains wax, which makes it extremely malleable and reusable. As ascertained by a number of researchers, such as Gad and Gao (2020), RP1 clay cannot be well described with simple constitutive models, as it exhibits both elastic and plastic behaviour, thus the mechanical properties vary with temperature, age, shear history, and loading rate. Consequently, at present, there is no agreement on material properties of RP1 clay which can be readily used for FE analysis (Roberts et al. 2007). To overcome this issue, several approaches have been applied to fit experimental data to existing material models. For example, Roberts et al. (2007) empirically calculated the non-linear properties of the clay using (quasi-static) drop tests, then used



**Figure 2.** Inverse method for material characterisation from drop testing (Hernandez et al. 2012).

numerical simulations to adjust the material properties of the clay until the FE model deformations matched the deformations measured experimentally. Shen et al. (2010) employed a combined experimental and modelling approach to quantify the deformation and energy transmission from ballistic impacts by comparing armour responses on gelatine or clay surrogate targets with those on a human torso FE model, where the material parameters used in the numerical model were selected to best fit model calculations to the test measurements.

Hernandez et al. (2012) proposed a mechanical characterisation method based on an inverse problem solved through an optimization procedure. In this method, the input data for the model was obtained from the penetration profile (i.e. the depth of cavity in the clay) of a steel sphere over time obtained from drop test experiments. The optimization process was employed to minimize the difference between the measured experimental data and the data computed by a reference model. The reference model is a finite element representation of the experimental test, and geometric moments are used for data reduction. The outcome of this process was the optimal set of material parameters, representing the material's behaviour under high strain rate conditions. This method provides a comprehensive approach to accurately characterise materials under dynamic loading conditions,

thus contributing valuable insights for various applications in materials science, impact analysis, and structural engineering. An overview of the method is depicted in Figure 2.

Kim et al. (2022a) used an inverse tracking method to determine the appropriate physical parameters that can capture the high-strain-rate behaviour of RP1 clay under impact without the need for any independent mechanical tests. The first step in this technique was to develop an FE model to predict the behaviour of RP1 clay under a number of different impact conditions in order to obtain the necessary training datasets (i.e. large datasets to teach the prediction model to extract the required information). Then, based on the results obtained from the numerical simulations, an Artificial Neural Network model was designed. The model was subsequently used to predict the response of the RP1 clay under various impact conditions, and an inverse tracking method was applied to select the optimal material parameters. Lastly, these optimal material parameters were input into the FE model for verification.

Gad and Gao (2020) employed a Johnson–Cook (J-C) material model in conjunction with a new constitutive model to computationally simulate the mechanical responses of RP1 clay from projectile impacts. The effects of strain rate and temperature were incorporated into both models to describe the plastic

deformation of RP1 clay. While the J-C model was obtained directly from the LS-DYNA library, a user-defined function was implemented in LS-DYNA for the new constitutive model. Kim et al. (2022b) used a different approach, employing a numerical model in conjunction with an empirical technique to understand the behaviour of RP1 clay under various impact conditions. The authors performed multiple drop tests with various configurations of indenter diameter, mass, and impact height in order to ascertain an empirical relationship between these parameters. A deep neural network prediction method was used to determine the physical input parameters related to the material model, and the application of this method led to improved accuracy of the numerical model.

Table 2 summarises the studies where different material models have been used to model RP1 clay. While there has been a range of material models employed to simulate the behaviour of RP1 clay, most of these were pre-existing models in the software Library, where the material properties only need to be entered to obtain the required output. While this has the obvious advantage of being easy to implement as the models can be directly extracted from LS-DYNA, these models do not fully represent the complexity of RP1 clay behaviour. This was demonstrated by Gad and Gao (2020), who compared the standard J-C model with a modified model, the New Constitutive Model (NCM). Gad and Gao (2020) found that while the standard J-C model could not fully capture the complex behaviour of RP1 clay, especially under conditions involving high strain rates and high temperatures, the NCM enabled a more customised and accurate representation of RP1 clay behaviour but had the limitation of requiring a complex user-defined algorithm to be developed and implemented. Similarly, the empirical approach employed by Kim et al. (2022a), which incorporates drop tests and deep neural network predictions, also enhances model accuracy by considering a wide range of impact conditions; however, it requires a considerable amount of experimental data for training the prediction model.

In the models which have been presented in the literature, the most frequent boundary condition (BC) employed for the clay block was to constrain the translational and rotational motion of nodes at the walls and base of the block in order to prevent motion of the clay during the impact, which is a reasonable assumption as the clay block is then considered to be rigid. However, for models where the projectile, clay and body armour have been combined, symmetry is the most commonly-used boundary

condition (BC) adopted, as it reduces the number of elements required for the model, thus saving computational time. Nevertheless, the symmetry BC involves reducing the whole structure to one-half or one-quarter of the full model geometry; thus, while this assumption is reasonable for the clay block, the symmetry BC means the model no longer represents the non-linear orthotropic behaviour exhibited by body armour. Consequently, for simulations involving the body armour, it is important to represent the whole impact area, and not reduce the model geometry in favour of computational time.

From the data in Table 2, it is apparent that most models have been validated using drop tests rather than higher-rate ballistic impacts. To simulate drop testing, most researchers have applied an initial velocity equivalent to that which would be reached after the ball or impactor has dropped a specific height; however, a gravitational load has also been occasionally included (Zochowski 2019; Chan 2021). Thus, it is apparent that in future research, one primary focus should be on model validation in order to improve the accuracy of RP1 clay simulations, particularly under high-rate ballistic impacts. This could involve designing experimental configurations that closely mimic real-world scenarios to ensure that the models accurately represent physical conditions. Additionally, the accuracy of these models can be enhanced by refining the characterisation of RP1 clay's material properties, accounting for variations in factors such as temperature and strain rate. Exploring advanced material models or hybrid approaches that amalgamate empirical data with physics-based models holds promise for achieving a more accurate representation of RP1 clay behaviour. Furthermore, considering more sophisticated boundary conditions that factor in non-linear orthotropic behaviour, especially in body armour simulations, has the potential to enhance the accuracy of FE models, providing a comprehensive foundation for future research in this domain. Additional details regarding some of the more complex methods can be found in Table 2.

### 3.3. Finite element models of the gelatine block

Ballistic gelatine, a mix of water and gelatine powder, has been widely used as a simulant for soft tissues in high-speed impact and penetration testing (Bodo et al. 2017; Bracq et al. 2017, 2018a, 2018b, 2019). By varying the concentration of the gelatine powder (10% or 20%), the density and mechanical properties of the test substance can be tailored to model various

Table 2. Finite element models of RP1 clay from the literature.

Reference	Software	Clay Material Model	Boundary conditions	Material Model	Validation
Rahbek (2015)	IMPETUS Afea	*MAT_VISCO_PLASTIC	<ul style="list-style-type: none"> <li>Symmetry in XZ-plane (Only half the model was considered)</li> <li>Clay walls were constrained from movements in all directions</li> <li>Gravitational force applied in z-direction.</li> <li>2D axisymmetric</li> </ul>	Non-linear visco-plastic constitutive model	<ul style="list-style-type: none"> <li>Drop test conditions</li> <li>Impactor = sphere, <math>d = 63.5</math> mm, <math>m = 1043</math> g</li> <li>Height = 2 m</li> <li>Velocity = 6.276 m/sec</li> <li>Clay block = <math>280 \times 280 \times 140</math> mm</li> </ul>
Kim et al. (2022a)	Ansys Autodyn	- EOS model & J-C model	<ul style="list-style-type: none"> <li>2D axisymmetric</li> </ul>	Not provided	<ul style="list-style-type: none"> <li>Drop and impact test conditions</li> <li>Impactor = different shapes, <math>d = 44.5</math> &amp; <math>63.5</math> mm, <math>m = 1000</math> and <math>1043</math> g</li> <li>Height = 2 m</li> <li>Velocity = 4.46 &amp; 6.26 m/sec</li> <li>Clay block = <math>400 \times 200</math> mm</li> <li>Drop and impact test conditions.</li> <li>Impactor = spherically headed cylindrical, <math>d = 44.5</math> mm, <math>m = 1000</math> g</li> <li>Height = 2 m</li> <li>Velocity = 6.1 to 55 m/sec</li> <li>Clay block = <math>360 \times 360 \times 140</math> mm</li> </ul>
Rahman (2013)	LS-DYNA	*MAT_005	<ul style="list-style-type: none"> <li>Symmetry in XZ-plane (Only half the model was considered)</li> <li>Clay walls and base were constrained from movements in all directions</li> </ul>	<ul style="list-style-type: none"> <li>This model simulates crushing through the volumetric deformations</li> <li>At very low yield stress this model gives nearly fluid like behaviour</li> </ul>	<ul style="list-style-type: none"> <li>Drop test = Cylindrical with spherical frontal part, <math>d = 44</math> mm, <math>m = 1000</math> g, Height = 2 m, Velocity = 6.2485 m/sec</li> <li>Ballistic test = <math>9 \times 19</math> mm Parabellum projectile</li> <li>Clay block = Not given</li> </ul>
Zochowski (2019)	LS-DYNA	*MAT_018	<ul style="list-style-type: none"> <li>Symmetry in XZ-plane and YZ-plane (only a quarter of geometry was modelled)</li> <li>Clay walls and base were constrained from movements in all directions</li> </ul>	Isotropic plasticity model with rate effects which uses a power law hardening rule.	<ul style="list-style-type: none"> <li>Drop test conditions at <math>T = 37</math> °C</li> <li>Impactor = spherically headed cylindrical, <math>d = 44.5</math> mm, <math>m = 1000</math> g</li> <li>Height = 2 m</li> <li>Velocity = 6.2485 m/sec</li> <li>Clay block = <math>280 \times 280 \times 140</math> mm</li> <li>Drop test = sphere, <math>d = 63.5</math>-mm, <math>m = 1000</math>-g, -Height = 2-m, -Velocity = 6.26-m/sec</li> <li>Ballistic test = .50 Cal FSP, <math>v = 530</math>-m/sec</li> <li>Clay block = <math>610 \times 610 \times 140</math>-mm</li> </ul>
Gad and Gao (2020)	LS-DYNA	- MAT_015 - Modified Johnson-Cook (J-C) Model was incorporated into the simulation via UDF	<ul style="list-style-type: none"> <li>Symmetry in XZ-plane and YZ-plane (only a quarter of geometry was modelled)</li> <li>Gravitational force was neglected.</li> </ul>	<ul style="list-style-type: none"> <li>This model requires the use of the equation-of-state</li> <li>This model used when strain rates vary over a large range and plastic heating cause material softening.</li> <li>The description of each model was provided in the previous references</li> </ul>	<ul style="list-style-type: none"> <li>Drop test conditions</li> <li>Impactor = sphere, <math>d = 63.5</math>, 50.8 &amp; 44.45 mm, <math>m = 357</math>, 535 &amp; 1045 g</li> <li>Height = 1, 1.5 &amp; 2 m</li> <li>Velocity = 6.276 m/sec</li> <li>Clay block = Not given</li> </ul>
Chan (2021)	LS-DYNA	- *MAT_064 - *MAT_015 - *MAT_005	<ul style="list-style-type: none"> <li>Symmetry in XZ-plane (Only half the model was considered)</li> <li>Clay walls and bottom were constrained from movements in all directions</li> <li>Gravitational force was considered in z-direction</li> </ul>	<ul style="list-style-type: none"> <li>Model follows a constitutive relationship</li> <li>User can control the magnitude of the pressure</li> </ul>	<ul style="list-style-type: none"> <li>Drop test conditions</li> <li>Impactor = sphere, <math>d = 63.5</math>, 50.8 &amp; 44.45 mm, <math>m = 357</math>, 535 &amp; 1045 g</li> <li>Height = 1, 1.5 &amp; 2 m</li> <li>Velocity = 6.276 m/sec</li> <li>Clay block = Not given</li> </ul>
Hernandez, Buchely, and Maranon (2015)	LS-DYNA	*MAT_064	<ul style="list-style-type: none"> <li>2D Axisymmetric model (XY-plane)</li> <li>Clay walls and bottom were constrained from movements in all directions</li> <li>Automatic 2D single surface</li> <li>Friction was considered at the contact point.</li> </ul>	<ul style="list-style-type: none"> <li>Model follows a constitutive relationship</li> <li>User can control the magnitude of the pressure</li> </ul>	<ul style="list-style-type: none"> <li>Drop test conditions</li> <li>Impactor = sphere, <math>d = 63.5</math>, 50.8 &amp; 44.45 mm, <math>m = 357</math>, 535 &amp; 1045 g</li> <li>Height = 1, 1.5 &amp; 2 m</li> <li>Velocity = 6.276 m/sec</li> <li>Clay block = Not given</li> </ul>

(continued)

Table 2. Continued.

Reference	Software	Clay Material Model	Boundary conditions	Material Model	Validation
Roberts et al. (2007)	LS-DYNA	*MAT_005	<ul style="list-style-type: none"> <li>Rigid wall conditions were imposed at bounding surfaces of the clay block.</li> </ul>	<ul style="list-style-type: none"> <li>Model simulates crushing through the volumetric deformations</li> <li>At very low yield stress model gives nearly fluid like behaviour</li> </ul>	<ul style="list-style-type: none"> <li>Drop test conditions</li> <li>Impactor = sphere, <math>d = 63.5</math> mm, <math>m = 104</math> g</li> <li>Height = 0.5, 1.0, 1.5 &amp; 2 m</li> <li>Velocity <math>\geq 6.21</math> m/sec</li> <li>Clay block = <math>610 \times 610 \times 140</math>-mm</li> </ul>
Zhang et al. (2017)	LS-DYNA	*MAT_124	<ul style="list-style-type: none"> <li>Friction effects between the clay and frames/plywood were ignored</li> <li>Symmetry in XZ-plane and YZ-plane (only a quarter of geometry was modelled)</li> <li>Base and walls of clay constrained normal to each surface.</li> </ul>	<ul style="list-style-type: none"> <li>Isotropic elastic-plastic material model</li> <li>Unique yield stress versus plastic strain curves can be defined for compression and tension in this model</li> </ul>	<ul style="list-style-type: none"> <li>Drop and impact test conditions</li> <li>Impactor = hemispherical nosed cylindrical, <math>d = 44.5</math> mm, <math>m = 1000</math> g</li> <li>Height = 2 m</li> <li>Velocity = 6.1 m/sec, velocity = 55 m/sec</li> <li>Clay block = Not given</li> </ul>

types of tissues, such as the brain and muscles (Cronin 2015; Cronin et al. 2018, 2021). Gelatine was initially employed in ballistic test standards as backing material, however, due to its high cost and the need to use high-speed imaging to track the deformation, clay was found to be a more affordable option with similar measurable post-test maximum BFD to gelatine (Cronin et al. 2001; Bustamante et al. 2019). Compared to clay, one major advantage of using ballistic gelatine is that the deformation profile can be expressed as a function of time; consequently, the speed at which the maximum depth is attained can be established, and the development of the BFD shape over time can also be ascertained (Cronin 2006, 2012).

The main limitation of gelatine is its high temperature sensitivity; therefore, it has to be cooled and then stored at a low temperature (about 4°C) to avoid deterioration. It also has the further disadvantage of not being reusable (Wen et al. 2013; Gilson et al. 2020). However, a number of researchers have recently started using new synthetic ballistic gelatines, which not only have a much longer shelf life than traditional gelatines, but do not undergo mechanical property degradation (Bodo et al. 2017; Bracq et al. 2018; Roth 2020).

As demonstrated in Table 3, which presents a summary of studies containing numerical models of ballistic gelatine which have been used to analyse BFD and BABT, software packages such as LS-DYNA, ABAQUS and RADIOSS have been employed to model the response of this substance. For most of these models, gelatine has been treated as a homogeneous isotropic elastic-plastic material. For instance, Zochowski (2019) applied the Elastic-Plastic-Hydrodynamic (\*Mat\_010) model available in LS-DYNA to simulate a gelatine calibration test and the penetration impact of  $7.62 \times 39$  mm PS (Púlya so Stal'ným serdéchnikom - i.e. bullet with a steal core) projectile on a gelatine block. Adopting this model, which requires the use of the equation-of-state (\*EOS), enabled an elastic-plastic hydrodynamic material with pressure dependant yield behaviour to be modelled. Wen et al. (2013), who also conducted simulations with a 7.62 mm PS projectile and an elastic-plastic material model for gelatine, found that there are two waves travelling in gelatine behind the armour: an initial compression wave resulting from the shock generated from the impact of the projectile on the armour, and a secondary distortion wave produced by the deformation and displacement of the armour. Another example where a homogeneous

**Table 3.** Finite element models of ballistic gelatine in literature.

Reference	Software	Boundary conditions	Gelatine Material Model	Material Model notes	Validation
Gilson et al. (2020)	LS-DYNA	Symmetry in XZ-plane and YZ-plane (only a quarter of geometry was modelled).	Elastic-plastic material with the polynomial EoS	<ul style="list-style-type: none"> <li>Rate effects not factored in model</li> <li>Gelatine assumed to be linear elastic, isotropic and homogeneous</li> </ul>	<ul style="list-style-type: none"> <li>Validated at ballistic test conditions</li> <li>Projectile = 9 mm Parabellum &amp; 0.44 Magnum</li> <li>Velocity = 390.25, 424.58 &amp; 1428 -m/sec</li> <li>Gelatin block = 155 × 140 × 290-mm</li> </ul>
Batra and Pydah (2020)	ABAQUS	Symmetry in XZ-plane and YZ-plane (only a quarter of geometry was modelled). No thermal BC's specified. No heat equation numerically solved	Not provided	<ul style="list-style-type: none"> <li>Elastic-plastic linearly strain-hardening material.</li> </ul>	<ul style="list-style-type: none"> <li>Validated at ballistic test conditions</li> <li>Projectile = Remington 40Cal</li> <li>Velocity = 180-m/sec</li> <li>Gelatine block = 100 × 100 × 10-mm</li> </ul>
Zochowski (2019)	LS-DYNA	Single symmetry plane	*MAT_010 *EOS_LINEAR_POLYNOMIAL	<ul style="list-style-type: none"> <li>Allows the modelling of an elastic-plastic hydrodynamic material and requires use of an*EoS</li> </ul>	<ul style="list-style-type: none"> <li>Validated at ballistic test conditions</li> <li>Projectile = 7.62 mm PS</li> <li>Velocity = 180-m/sec</li> </ul>
Ye et al. (2022)	LS-DYNA	2D axisymmetric	Not provided	<ul style="list-style-type: none"> <li>Gelatine was modelled as an isotropic and homogeneous elastic-plastic material</li> <li>Polynomial EoS was used</li> </ul>	<ul style="list-style-type: none"> <li>Validated at ballistic test conditions</li> <li>Projectile = spherical steel, <math>d = 1</math> to 5-mm</li> <li>Velocity = 50 to 400-m/sec</li> <li>Gelatine block = 72 × 155-mm</li> </ul>
Choudhury et al. (2022)	ABAQUS	The gelatine block was constrained from movements in all directions	Not provided	<ul style="list-style-type: none"> <li>Gelatine assumed to be linear elastic, isotropic and homogeneous</li> </ul>	<ul style="list-style-type: none"> <li>Validated against analytical model</li> <li>Projectile = spherical steel, <math>d = 1</math> to 5-mm</li> <li>Velocity = 25 to 175-m/sec</li> <li>Gelatine block = Not provided</li> </ul>
Shen, Taddei, and Roth (2022)	RADIOSS	Symmetry in XZ-plane and YZ-plane (only a quarter of geometry was modelled). Gelatine walls and bottom were constrained from movements in all directions	A new constitutive law model was implemented into the simulation as UDF	<ul style="list-style-type: none"> <li>Hydrodynamic behaviour was represented by a polynomial*EoS</li> </ul>	<ul style="list-style-type: none"> <li>Validated with tests using a blunt impactor to represent BFD</li> <li>Projectile = cylindrical, <math>d = 16.1</math>-mm</li> <li>Velocity = 12, 20 &amp; 30-m/sec</li> <li>Gelatine block = Dimensions of block not provided</li> </ul>
Bracq et al. (2020, 2019)	RADIOSS	Symmetry in XZ-plane and YZ-plane (only a quarter of geometry was modelled). Projectile is considered as rigid	Not provided	<ul style="list-style-type: none"> <li>Visco-hyperelastic model</li> </ul>	<ul style="list-style-type: none"> <li>Validated at ballistic test conditions</li> <li>Projectile = Remington 40Cal, RWS 38 special &amp; Federal Premium 40 Cal</li> <li>Velocity = 295.4, 262.2 &amp; 297.3-m/sec</li> <li>Gelatine block = 250 × 250 × 250-mm</li> </ul>
Wen et al. (2015)	LS-DYNA	Symmetry in XZ-plane and YZ-plane (only a quarter of geometry was modelled).	Not provided	<ul style="list-style-type: none"> <li>Gelatine modelled as a strain-rate dependent hyperelastic material.</li> </ul>	<ul style="list-style-type: none"> <li>Validated at ballistic test conditions</li> <li>Projectile = 7.62 mm PS</li> <li>Velocity = 400 to 900-m/sec</li> <li>Gelatine block = 300 × 300 × 300-mm</li> </ul>

\*EoS = Equation of State; UDF = User Defined Function.

isotropic elastic-plastic gelatine material model was employed is described in the study by Ye et al. (2022), who developed an FE model to simulate experimental observations of the penetration dynamics of ballistic gelatine. Using spherical steel projectiles of varying diameters impacting the gelatine at different incident velocities, the simulation involved tracking the displacements, velocities, and stresses of the projectiles within the gelatine as a function of time. The results demonstrated that there was a power-law relationship between the kinetic energy of the projectiles and the maximum penetration at high incident velocities, but not at intermediate and low velocities.

Other homogeneous isotropic elastic-plastic gelatine material models include those developed by Choudhury et al. (2022) and Gilson et al. (2020). Choudhury et al. (2022) used gelatine to represent the torso, using both an analytical methods and FE analysis to simulate three different cases of a projectile impacting body armour shielding the gelatine block, where the body armour had: 1) no backing material, 2) a rubber backing material and 3) an air gap. Calculating the Viscous Criteria (VC max) and the Stored Energy Criteria (SEC) criteria from the gelatine in order to predict BABT, the authors found that both a rubber backing, or an air gap, can significantly mitigate BABT compared to impacts where no backing or gap is used, with rubber backings showing superior performance to air gaps due to higher energy absorption and greater injury mitigation.

Gilson et al. (2020) employed both experimental and numerical approaches to investigate the non-penetrating ballistic response of gelatine blocks shielded by a composite plate. The experimental tests involved using pressure gauges to record the transient pressures and a high-speed camera to capture the transient BFD profiles, while the numerical analysis was comprised of developing an FE model to assess the front face deformation of the gelatine blocks, the pressure wave amplitude, and duration of the pressure wave. The authors found the presence of pressure waves propagating after the ballistic impact, where the pattern of pressure waves was influenced by a number of factors, such as the type of projectile used.

Alternative approaches to model gelatine include the new constitutive law model presented by Shen and colleagues (Shen, Taddei, and Roth 2022), which requires a complex user-defined function to be added to software package rather than the use of a pre-existing material algorithm from the software package library. For example, in this particular instance, Shen, Taddei, and Roth (2022) proposed an elasto-

hydrodynamic constitutive law to describe the mechanical behaviour of synthetic polymer SEBS gel, and the material model was then implemented into an explicit non-linear FE software package to simulate various loading conditions. The numerical results revealed that the strain-rate-dependence effect in SEBS gel is significant, especially at high strain rates. Bracq et al. (2020) developed a visco-hyperelastic gelatine model, validating it at ballistic test conditions, in order to use the BFD data from their gelatine model as the input to the HUBYX torso model, which was developed by another group.

As in the case of RP1 clay, the most common BC which has been used for numerical models of ballistic gelatine is symmetry. Unlike body armour, which exhibits orthotropic behaviour, ballistic gelatine is similar to clay in that reducing the model geometry due to a symmetry BC is a reasonable approach as gelatine can be regarded as isotropic in behaviour.

Unlike clay-based computational models which have been predominately validated using lower-speed drop tests, FE models of gelatine have been extensively validated under high-speed ballistic impact conditions. With the exception of the model by Shen, Taddei, and Roth (2022), all the models described in Table 3 have been validated by simulating ballistic experiments of a projectile impacting body armour placed over a gelatine block. Shen and colleagues conducted an alternative validation method by simulating experimental tests of a blunt cylindrical impactor striking the gelatine block at impact velocities intended to replicate blunt impact BFD experienced by the torso. The difference in validation methods between clay and gelatine FE models highlights the broader range of scenarios and wider range of applications gelatine models are suitable for, as they have been tested under more dynamic real-world conditions than clay-based models.

### 3.4. Finite element models of the human torso

Assessing and predicting the effects of BFD on the human body as result of non-penetrating projectile impacts into armour is highly challenging, as experimental testing on living humans is limited to specific scenarios and impact velocities, for example, volunteers cannot be tested at an impact velocity which will result in injuries. Alternatively, ballistic testing can be performed on cadavers or living animals (Ndompetelo 2016; Gilson et al. 2021), but each of these methods also have a number of disadvantages. For example, while cadavers have the same anatomical structure

and mass distribution of a living human, they are unable to replicate the resulting physiological cascade from an impact over time; thus, their use is limited to evaluating the injuries sustained from the acute traumatic event. Furthermore, they cannot simulate the dynamic muscle responses of living subjects, and do not fully reproduce the response of living tissues due to early post-mortem changes such as primary muscle relaxation and loss of skin elasticity (Shedge et al. 2023), both of which can alter energy transfer through the tissues. Lastly, the complex kinematics which living humans are subjected to during an impact cannot be fully re-created with cadaveric subjects, a factor which may affect the severity of trauma sustained.

There are also significant limitations with animals as an experimental subject. For example, while the physiological responses from trauma can be monitored in living animals under anaesthesia, the results from these experiments are difficult to scale to humans due to differences in physiology and anatomy. A further disadvantage of both cadavers and living animals is that testing with these surrogates is neither repeatable nor reproducible. Thus, biofidelic numerical techniques are an alternative method to study BABT, and while there have been a growing number of human torso models developed over the last few decades (Table 4), most of these have been for blunt impact (i.e. automotive-based models used for military scenarios), with only a few models developed exclusively for ballistic BFD applications.

#### ***Civilian-based models used for military studies***

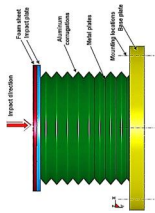
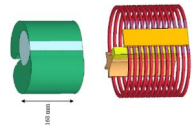
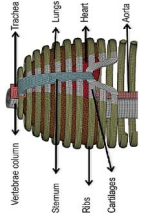
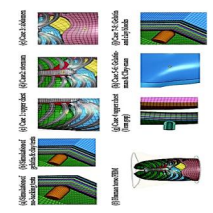
One of the simplest torso FE models available in the literature, the Mechanical THORax for Trauma Assessment (MTHOTA), was developed to emulate the thorax model developed by Wayne State University. Comprised of a series of collapsible aluminium corrugations separated by a series of metal panels, the entire structure is sandwiched between two external plates: a base plate and an impact plate (MurthyThota, Eeparachchi, and Lau 2012; Thota, Eeparachchi, and Lau 2014a, 2014b). The model was validated with the thoracic force – time response from a 50<sup>th</sup> percentile male Hybrid III anthropomorphic test device (ATD) under high speed (50–100 m/s) low mass (27.3-gram, 40 mm projectile) impact conditions using Bir's (Bir 2000) biomechanical corridors and projectiles. However, it is worth noting that the model's reliance on a non-manufacturable corrugated aluminium sheeting and its limited validation for specific parameters, such as a minimal number of loading conditions, may raise concerns

about its applicability to a wider range of real-world thoracic injury scenarios.

Slightly more detailed than the MTHOTA, Bouamoul and Lévesque's simplified three-dimensional human torso model (Bouamoul and Lévesque 2007), which was denoted the 'Waterloo Model', contains a number of internal chest organs, including the heart and lungs, encased by a skeletal ribcage structure. Simulations were performed impacting the model with non-compressible polyvinyl chloride cylinders 37 mm in diameter, which were either 28.5 mm or 100 mm long. The predicted results of the chest dynamic deflection, the dynamic force applied on the chest and the force applied on the chest as a function of chest deflection were compared the results of ballistic blunt impact experiments on cadavers from Bir (2000). While there was some agreement between the model and experimental results, in the model, the deflection peak was earlier, and was lower in magnitude, than the experimental data. However, it is important to note that this model, like the MTHOTA, contains limitations, including discrepancies in replicating the exact timing and magnitude of thoracic deflection observed in experiments, and potential oversimplification of geometry and material properties, both factors of which may restrict its broader applicability to real-world scenarios.

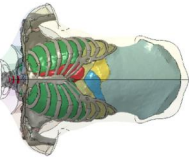
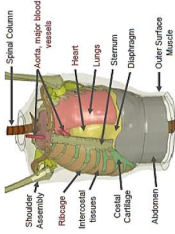
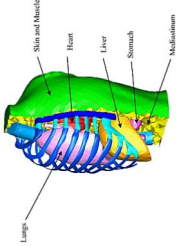
Another simplified model, the Surrogate Human Thorax Impact Model (SHTIM), was proposed by Ndompetelo (2016) as part of PhD project. The model has been employed as a tool for injury risk assessment of non-penetrating thoracic impacts due to non-lethal projectiles, and rather than being based on standard 50<sup>th</sup> percentile male anthropometry, it contains approximate representations of the thorax's principal organs. The model comprises the thoracic skeletal structure (sternum, vertebrae, and 12 pairs of ribs), the heart, the lungs, the costal cartilages, intercostal muscles, the fatty tissues, and the skin. Several simplifications were made to reduce the computational time and the complexity of the model, for example, the diaphragm was not included, while voids between organs in the thoracic cavity such as fluid, blood vessels and other internal tissues were not factored. In addition, the ribs were modelled with a constant cross-sectional area rather than actual rib anatomy, where each rib has a varying cross-sectional area along its curvature. While this model remains an invaluable tool for assessing injury risk from non-lethal projectiles, it is important to recognise that the simplifications discussed above, including the exclusion of some internal structures, reduce the

**Table 4.** Thorax FE models for blunt impact injury research.

Authors	Model Name	Software	Anthropometry	Model Figure	Material Models	Validation	Further Details
<b>Civilian-based models</b> Murthy/Thota, Epaarachchi, and Lau (2012), Thota, Epaarachchi, and Lau (2014a, 2014b)	MITHOTA (Mechanical THORax for Trauma Assessment) Model	LS-DYNA	$d = 300$ mm $h = 180$ mm 50 <sup>th</sup> percentile male Civilian Anthropometry		Foam sheet = *MAT_057 Impact plate = *MAT_001 Corrugations = *MAT_003 Metal plates = *MAT_003	<ul style="list-style-type: none"> <li>Surrogate of the Hybrid III 50th percentile male rigid dummy was used in pilot study</li> <li>Bir's blunt and ballistic thoracic impact data (Bir 2000)</li> <li>Velocity range = 50 - 100 m/s</li> </ul>	<ul style="list-style-type: none"> <li>Developed by University of Southern Queensland, Australia</li> <li>Was developed for numerical evaluation of the KENL#</li> <li>The model consists of seven components (foam sheet, rigid impact plate, corrugated sheet, 4 plates)</li> <li>Not commercially available</li> <li>Developed by the University of Waterloo, USA</li> <li>Not commercially available</li> </ul>
Bouamoul and Lévesque (2007)	Waterloo Model	LS-DYNA	$h = 168$ mm		<b>Internal organs/soft tissue</b> <ul style="list-style-type: none"> <li>Heart, Muscle, Intercoastal &amp; Internal tissue = *MAT_181</li> <li>Lungs = *MAT_009</li> <li>Skin = Not included</li> </ul> <b>Skeletal structure</b> <ul style="list-style-type: none"> <li>Ribs, Sternum, Cartilage &amp; Vertebrae = *MAT_001</li> </ul> <b>Internal organs/soft tissue</b> <ul style="list-style-type: none"> <li>Heart, Flesh*, Aorta &amp; Trachea = *MAT_181</li> <li>Lungs = *MAT_129</li> </ul> <b>Skeletal structure</b> <ul style="list-style-type: none"> <li>Ribs, Sternum, Cartilage &amp; Vertebrae = *MAT_005</li> <li>Flesh = Flesh, Skin, Muscles &amp; Internal tissue</li> </ul> <b>Internal organs/soft tissue</b> <ul style="list-style-type: none"> <li>Skin, muscles, &amp; abdominal organs = incompressible, hyper-elastic, and viscoelastic</li> <li>Lung = hyperplastic</li> </ul> <b>Skeletal structure</b> <ul style="list-style-type: none"> <li>Ribs and Cartilages = modelled as inhomogeneous beams</li> </ul>	<ul style="list-style-type: none"> <li>Bir's blunt and ballistic thoracic impact data (Bir 2000)</li> </ul>	<ul style="list-style-type: none"> <li>Developed by the University of Waterloo, USA</li> <li>Not commercially available</li> </ul>
Ndempetelo (2016)	SHTIM (Surrogate Human Thorax Impact Model) Model	LS-DYNA	Approximate representation of the principal organs of the male thorax		<ul style="list-style-type: none"> <li>Heart, Flesh*, Aorta &amp; Trachea = *MAT_181</li> <li>Lungs = *MAT_129</li> </ul>	<ul style="list-style-type: none"> <li>Bir's blunt and ballistic thoracic impact data (Bir 2000)</li> </ul>	<ul style="list-style-type: none"> <li>Model consists of 12 pairs of ribs, the sternum, spine and vertebrae</li> <li>Developed as part of PhD thesis and not commercially available</li> </ul>
Shen et al. (2008)	ATBM (Advanced Total Body Model)	LS-DYNA	95 <sup>th</sup> percentile male Civilian Anthropometry		<ul style="list-style-type: none"> <li>Skin, muscles, &amp; abdominal organs = incompressible, hyper-elastic, and viscoelastic</li> <li>Lung = hyperplastic</li> </ul>	<ul style="list-style-type: none"> <li>Cadaveric impact tests at high loading rate compatible to bullet armour loading.</li> <li>Historical PMHS test data (Kroell, Schneider, and Nahum 1971, Viano et al. 1989).</li> </ul>	<ul style="list-style-type: none"> <li>Developed using the CT data set from the Visible Human project</li> <li>Model can be scaled to fit different anthropometry</li> <li>Not commercially available</li> </ul>

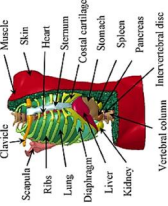

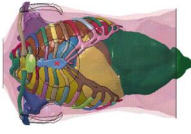
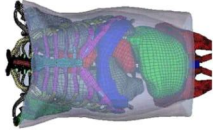
(continued)

Table 4. Continued.

Authors	Model Name	Software	Anthropometry	Model Figure	Material Models	Validation	Further Details
Ng and Niu (2018)	ATBM Model (Other researchers at same institution developed this model later, using same name as previous model)	LS-DYNA	50 <sup>th</sup> percentile male Civilian Anthropometry		<p><b>Internal organs</b></p> <ul style="list-style-type: none"> <li>Lung = Viscoelastic</li> <li>Liver, Stomach, intestine interior &amp; Spleen = Ogden rubber</li> <li>Heart = Elastic</li> <li>Blood Vessels = Elastic fluid</li> </ul> <p><b>Skeletal structure</b></p> <p>Sternum, Vertebral, Disc, Scapula, Clavicle &amp; Humerus = Elastic</p>	<ul style="list-style-type: none"> <li>Frontal impact cadaveric tests</li> </ul>	<ul style="list-style-type: none"> <li>Anatomy from the Zygote 3D Human Male which they scaled to develop a number of subject-specific FE models 50 - 75 kg for validation against cadaveric tests, with the final model being 50th percentile.</li> <li>The final version of FE model yet to complete</li> <li>The model was developed by L-3 Applied Technologies, USA</li> <li>Not commercially available</li> </ul>
Cronin (2006, 2012, 2015), Cronin et al. (2001, 2018, 2021)	BABT-WALT (Waterloo Thorax) Model	LS-DYNA	50 <sup>th</sup> percentile male Civilian Anthropometry		<p><b>Internal organs/soft tissue</b></p> <ul style="list-style-type: none"> <li>Heart = *MAT_128</li> <li>Lungs = *MAT_129</li> <li>Muscles = *MAT_181</li> </ul> <p><b>Skeletal structure</b></p> <ul style="list-style-type: none"> <li>Ribs = *MAT_019</li> <li>Costal cartilage = *MAT_006</li> <li>Sternum = *MAT_003</li> </ul>	<ul style="list-style-type: none"> <li>Corridors of the thorax to blunt ballistic impacts (Bir, Viano, and King 2004).</li> </ul>	<ul style="list-style-type: none"> <li>Developed by Waterloo University, Canada</li> <li>Model initially designed for automotive applications, and was then improved to model BABT Loader Plate (LP) method was used to represent BFD history</li> <li>Not commercially available</li> </ul>
Roberts, O'Connor, and Ward (2005)	HTFEM Model	LS-DYNA	5 <sup>th</sup> percentile male		<p><b>Internal organs &amp; viscera</b></p> <ul style="list-style-type: none"> <li>Viscoelastic</li> </ul> <p><b>Bone</b></p> <ul style="list-style-type: none"> <li>Linear elastic</li> </ul>	<ul style="list-style-type: none"> <li>Four impacts simulated against NIJ level II and level IIIa KEVLAR vests</li> <li>Projectile = 9 mm bullet at speed of 360 &amp; 425 m/sec</li> </ul>	<ul style="list-style-type: none"> <li>Developed by APL, Johns Hopkins University, USA</li> <li>Thoracic data of human male obtained from Viewpoint-Draper software</li> <li>Model was used to compare data with a physical human surrogate developed concurrently</li> <li>Not commercially available</li> </ul>

(continued)

Table 4. Continued.

Authors	Model Name	Software	Anthropometry	Model Figure	Material Models	Validation	Further Details
Tang et al. (2019)	—	LS-DYNA	50 <sup>th</sup> percentile male Civilian Anthropometry		<p><b>Internal organs/soft tissue</b></p> <ul style="list-style-type: none"> <li>• Skin = *MAT_022</li> <li>• Internal organs &amp; Muscle = *MAT_006</li> </ul> <p><b>Skeletal structure</b></p> <ul style="list-style-type: none"> <li>• Diaphragm &amp; Skeletons = *MAT_022</li> </ul>	<ul style="list-style-type: none"> <li>• Experimental data of human chest response to the Luger ammo (430 m/s) and Kevlar body armour (10.82 mm) (Roberts et al. 2007).</li> </ul>	<ul style="list-style-type: none"> <li>• Model was developed by Beijing Institute of Technology, China</li> <li>• Model was developed using data from CT, MRI &amp; MIMICS.</li> <li>• Not commercially available</li> </ul>
<b>Military-based models</b> Zochowski (2019)	—	LS-DYNA	50 <sup>th</sup> percentile male Military Anthropometry		<p><b>Internal organs/soft tissue</b></p> <ul style="list-style-type: none"> <li>• Skin, Diaphragm, &amp; Some internal organs = *MAT_001</li> <li>• Muscles = *MAT_006</li> </ul> <p><b>Skeletal structure</b></p> <ul style="list-style-type: none"> <li>• Bones = *MAT_003</li> </ul>	<ul style="list-style-type: none"> <li>• Bir's blunt and ballistic thoracic impact data (Bir 2000)</li> <li>• Frontal impact cadaveric tests (Kroell, Schneider, and Nahum 1971).</li> <li>• Lateral impact cadaveric tests (Chung et al. 1999).</li> <li>• Abdominal frontal impact cadaveric tests (Cavanaugh et al. 1986).</li> </ul>	<ul style="list-style-type: none"> <li>• Developed by the Military Institute of Armament Technology, Poland</li> <li>• Created in Altair Hypermesh using CT scan data of human male</li> <li>• Not commercially available</li> </ul>
Hampton and Kleinberger (2018a)	ARL Model	LS-DYNA	50 <sup>th</sup> percentile male Military Anthropometry		<p><b>Fluids</b></p> <ul style="list-style-type: none"> <li>• Blood, Air &amp; other Body Fluids = *MAT_001</li> </ul> <p>Different material models were tested.</p> <p><b>Internal organs/soft tissue</b></p> <ul style="list-style-type: none"> <li>• Internal Organs = *MAT_057, *MAT_062, *MAT_092 &amp; *MAT_077</li> </ul> <p><b>Skeletal structure</b></p> <p>All Bones = a single type of homogenous material</p>	<ul style="list-style-type: none"> <li>• Experimental data of human chest response to blunt impact using unembalmed cadavers (Backaitis 1994).</li> <li>• Frontal impact cadaveric tests (Kroell, Schneider, and Nahum 1971).</li> </ul>	<ul style="list-style-type: none"> <li>• Developed by Army Research Laboratory, USA</li> <li>• Anatomy from the Zygote 3D Male Human Model</li> <li>• Can be used with ParaDyn, Sierra, and ALE3D</li> <li>• Not commercially available</li> </ul>
Roth et al. (2013)	HUBYY Model	RADIOSS	50 <sup>th</sup> percentile male Military Anthropometry		<p><b>Internal organs</b></p> <ul style="list-style-type: none"> <li>• Aorta, Trachea, Diaphragm, Muscles, Skin, Inter-organs space/fat and Abdomen/ Intestine = Elastic</li> </ul> <p><b>Soft tissues</b></p> <ul style="list-style-type: none"> <li>• Viscoelastic</li> </ul> <p><b>Skeletal structure</b></p> <ul style="list-style-type: none"> <li>• Spongy bone, Cartilage &amp; Intervertebral disc = Elastic</li> <li>• Cortical bone = Elastic-plastic</li> </ul>	<ul style="list-style-type: none"> <li>• Bir's blunt and ballistic thoracic impact data (Bir 2000)</li> <li>• Experimental data of frontal and side impact crash tests (Kroell, Schneider, and Nahum 1971).</li> </ul>	<ul style="list-style-type: none"> <li>• Model was developed by CEDREM centre, France</li> <li>• Created using CT scans of thorax/abdomen/pelvis system</li> <li>• Model is commercially available</li> </ul>

\*KLENL: Kinetic Energy Non-Lethal.

anatomical biofidelity of the model. While this offers a practical benefit in terms of enhanced computational efficiency, reducing the complexity of the model potentially affects its accuracy when simulating intricate thoracic responses to impact, potentially constraining its broader applicability.

More advanced civilian-based models have been developed using CT scans of human subjects to obtain detailed geometrical data, and include the main thoracic and abdominal organs such as the heart, lungs, kidneys, and liver enclosed by a skeleton. For example, using the 3D-DOCTOR software to reconstruct the raw anatomies of the rib cage and soft organs from CT images of a human subject, Shen et al. (2008) developed a detailed 50<sup>th</sup> percentile human thorax and abdominal model containing approximately 77,000 nodes, 3,000 beam elements, 18,000 shell elements, 47,000 solid elements, and 450,000 total DOFs. Denoted the Advanced Total Body Model (ATBM) and validated against historical frontal and side-impact cadaveric tests from the literature, the model was then used to predict a variety of injuries such as rib fractures, lung contusions, pneumothoraces, heart lesions, and skin penetrations. The model showed significant progress and promise in predicting thoracic responses to high-speed blunt impact, which can have applications in understanding and preventing trauma. Nevertheless, it had some limitations related to accurately quantifying soft tissue injuries, primarily due to the limited number of soft tissue injuries sustained by the cadavers in the experimental tests.

The ATBM, developed by Ng and Niu (2018) was designed to predict torso responses from blunt impacts, including motion, stresses, and strains of the thorax region. Somewhat confusingly, the model was denoted the same name and abbreviation as the earlier torso model created by Shen et al. (2008), having been developed at the same organisation as the previous model. The geometry of the Ng and Niu (2018) model was derived from the Zygote anatomical model, developed by the Zygote Media Group Inc., which is assumed to be representative of a 50th percentile civilian male. The model contains tissue (bones, organs, and flesh i.e. muscle and skin), and was discretised at the organ level using HyperMesh, containing a total of 129 parts, 6,971,258 solid elements, 6,765,273 shell elements, 3,222 beam elements and 1,269,774 nodes. The ATBM was assigned tissue material properties from the literature and validated using cadaveric tests from the Medical College of Wisconsin (MCW). In the MCW experiments, which

were performed in 2017, the weights of the subjects ranged from 50 to 75 kg, and projectiles from 62.6 and 72.9 grams were fired at the cadavers at impact speeds ranging from 67.3 to 86.4 m/s. For the validation, the torso FE model was scaled to match the mass of the cadavers. The force-time histories for impacts to the intestine, stomach, and kidney obtained from the FE model were compared to the test data, where Ng and Niu (2018) found a good correlation between the simulations and the experiments. The ATBM was able to predict both gross and micro-level dynamic responses of a 50<sup>th</sup> percentile male's torso during high-speed non-lethal weapon (NLW) impacts, where the responses were used to predict organ injuries within the torso region. Thus, the model represents a significant step forward in accurately predicting torso responses to blunt impacts and provides valuable insights for injury mitigation strategies. However, while the model could predict stresses and strains within the organs, the authors did not correlate these with injury potential. Additionally, it had a number of limitations, including the exclusion of certain anatomical elements, such as minor blood vessels and tendons.

The BAPT-WALT (BAPT-Waterloo Thorax) model, developed by Cronin et al. (2021), was initially designed for automotive impacts, but later extended into military applications. The model comprises a detailed thoracic cage, the musculature, and the main internal organs such as the heart and lungs; but does not include skin or blood vessels. The numerical accuracy of the model was enhanced from the initial automotive version by improving the costal cartilage properties, using a refined mesh at the impact locations, and including wave-effects (Cronin 2006) as well as high-deformation-rate material properties (Bir, Viano, and King 2004). The failure criteria and the mechanical properties of the sternum and ribs were also improved in order to predict fracture initiation. While the BAPT-WALT model was initially validated using automotive-rate cadaveric data (Bir, Viano, and King 2004; Campbell and Cronin 2014), additional validation of the model for BFD impacts was later performed using the Less Lethal Kinetic Weapons (LLKE) cadaveric database (Bir, Viano, and King 2004), where the model was used to simulate BFD events (Cronin 2006; Cronin et al. 2021). The values predicted from the model matched BFD results observed for ballistic impacts at 20 and 40 m/s from the LLKE cases, but the BAPT-WALT had a stiffer response for the 60 m/s impacts than the response from the cadaveric tests (Bir, Viano, and King 2004).

Nevertheless, the level of BFD validation for the model highlights its potential as an invaluable tool for evaluating the effect of BFD-induced blunt trauma, aligning well with the goals of understanding and mitigating BAPT injuries. The latest version of BAPT-WALT thorax model contains 402,068 solids hexahedral, 36,536 shell, and 930 beam elements, but is not commercially available.

The Human Torso Finite Element Model (HTFEM), another complex model, was developed in LSDYNA to simulate non-penetrating ballistic impacts to a 5th percentile male torso (Roberts, O'Connor, and Ward 2005, Roberts et al. 2007). Although the authors obtained a complete anatomical dataset of the human subject using the Viewpoint software; only the thorax was simulated in the HTFEM, with the torso skeletal system, complete torso musculoskeletal structure, skin, heart, respiratory and digestive systems included in the model. The HTFEM model comprises 112,646 solid elements and 4,590 4-noded membrane shell elements, where linear tetrahedral solid elements were employed to simulate skeletal structure, organs, and mediastinum, and the membrane elements were used for meshing the peripheral musculature and skin. In this model, the internal organs do not share nodes, but they transfer load through defined contact interfaces between the various components, thus allowing a slip boundary condition at the interface between the organs as well as between the organs and the skeletal structure. A low coefficient of friction (0.0003) was adopted between organs to enforce the slip condition for elements. Two types of soft armour vests (NIJ level II and level IIIa KEVLAR®) under different ballistic impact conditions were simulated, and the model was then used to predict the peak pressures and kinetic energy in the organs. This model has contributed significantly to the current understanding of thoracic responses to ballistic impact, offering a valuable tool for evaluating body armour design, injury mitigation, and injury mechanisms.

Using CT and MRI to obtain geometrical data, Tang et al. (2019) developed a detailed human torso model comprising multiple organs to predict the mechanical response (i.e. the distributions of stress and pressure) of the tissues under blunt ballistic pistol cartridge impacts. The model represents a male 178 cm in height and weighing 70 kg, and includes the skeletal structure, skin, muscle, and internal organs of the torso. The skin was meshed with 23,251 Belytschko-Tsay shell elements, while the internal organs, skeleton and muscle contained 1,766,341

tetrahedral elements. The model was validated using experimental data of human chest responses to Luger ammunition (velocity = 430 m/s) fired at Kevlar body armour which had a thickness of 10.82 mm (Roberts et al. 2007). Overall, this comprehensive torso model represents a valuable asset in advancing current knowledge of blunt trauma mechanisms and enhancing the development of effective injury mitigation strategies for body armour applications.

While the models discussed above offer valuable insights into the dynamics of blunt trauma, they are not without limitations. Many of the simpler models, such as the MTHOTA and the Waterloo Model, exhibit discrepancies in replicating the exact timing and magnitude of thoracic deflections observed in experiments. Moreover, the geometric and material property oversimplifications in conjunction with not accounting for inter-individual variability in thoracic responses can limit their broader applicability to real-world scenarios and clinical contexts. Even more complex models like the SHTIM and HTFEM, while offering significant advancements in biofidelity, have limitations in anatomical detail, excluding some internal structures in order to prioritise computational efficiency. Nevertheless, the more complex models still require high computational demands; thus, this must be weighted against the need for more precise anatomical detail and factors such as accurate material property characterisation before choosing a model for a specific application.

Additionally, it is important to acknowledge several limitations associated with these advanced models, particularly those developed using civilian anatomical data. For instance, both ATBM and the BAPT-WALT model were developed using civilian anthropometry, and thus may not represent the body sizes and dimensions of military personnel. The variability in anthropometry between civilian and military populations could introduce differences in injury predictions, and consequently injury mitigation strategies, potentially impacting the applicability of these models to military-specific scenarios. Thus, while these models have significantly advanced the current understanding of blunt trauma mechanics, the fact that they were developed from civilian data is an important consideration when translating their findings to military contexts.

### ***Military-based models***

The majority of FE models of the torso have been developed and validated for automotive impacts; thus, there are only a handful of FE models specifically

designed for military applications such as BFD. One of the least complex of these models, developed by the Military Institute of Armament Technology in Poland, is a whole-body FE model created from CT scans of a 30-year-old male with a height of 180 cm and weight of 80 kg to represent a military combatant (Zochowski 2019). Using Altair Hyperworks to generate the geometry of organs and Hypermesh for discretisation of the two-dimensional mesh, the model was then solved using LS-DYNA. It includes a complete skeletal structure, a detailed representation of all principal internal organs, soft tissues, the musculature, and the skin, with 200,000 8-noded solid elements, 22,000 4-noded quadrilateral shell elements and approximately 162,000 Smoothed Particle Hydrodynamics (SPH) particles to represent the internal fluid. SPH particles were also used to fill the hollow organs as well as the cavities between the organs. Both trabecular and cortical bone were also represented. The model was validated against a series of cadaveric tests, including blunt impact frontal Kroell, Schneider, and Nahum (1971) and lateral Chung et al. (1999) pendulum tests, and lower mass, higher velocity impact experiments designed to replicate armour BFD (Cavanaugh et al. 1986; Bir 2000), where the authors were able to obtain reasonable correlations between their model and the experimental data. Thus, while the model has been subjected to a considerable amount of validation, its main drawback lies in its limited validation involving low-mass high-velocity projectiles designed to replicate armour BFD. Consequently, supplementing the validation, both with additional low-mass high-velocity projectile cadaveric tests and real-world impact data, would greatly strengthen this model.

The Hermaphrodite Universal Biomechanical YX model (HUBYX) (Roth et al. 2013), developed by a group of French researchers to predict injuries from ballistic impacts, blast events and BFD, was initially created from CT scans of the thorax/abdomen/pelvis systems from 12 subjects before the full geometries were reconstructed from the scans using Altair Hyperworks. The geometries were then compared with the data from the literature in order to select the anatomy which best represented a 50<sup>th</sup> percentile male, based on a NASA model of space module crew members. The final model included the skeletal system of the torso (vertebrae, intervertebral discs, ribs), the main internal organs of the human thorax (heart, lungs, kidneys, liver, spleen, stomach, intestines), the musculature, and the skin. The HUBYX model was created in Altair Hypermesh then solved using

RADIOSS, and includes 233,000 SPH particles, 77,800 4-nodes shell elements and 38,600 8-nodes brick elements. The experimental data from Bir (2000) was used to validate the model in terms of deflection and force. The HUBYX has also been used in a study by Bracq et al. (2020), who developed their own gelatine FE model (mentioned earlier), then used the BFD data from their model to apply to the thorax of the HUBYX, correlating the energy from the gelatine model with the probability of rib fractures according to anthropometric data and impact locations. The numerical pressure values of the impacted lung were also computed, which can be related to lung contusions; however, there was insufficient data for the authors to establish an injury risk curve. In summary, the HUBYX model is valuable tool for studying rib dynamics and rib fractures, especially in high-velocity impact scenarios. Its level of validation makes it a promising model for biomechanical research. However, users should be aware of its sensitivity to material properties and the need for careful consideration of model parameters to ensure accurate results under specific types of impacts. The HUBYX is commercially available as part of Altair Hyperworks software.

The ARL torso FE model, another model specifically designed for ballistic applications, was developed by Hampton and Kleinberger (2018a, 2018b) and represents a 21-year-old 50<sup>th</sup> percentile human male, where the geometrical data was derived from the Zygote anatomical model, developed by the Zygote Media Group Inc. The ARL model has a complex design where the bones, muscles, and skin were treated as separate components and meshed individually using the ICEM CFD (ANSYS) meshing software before the meshes were connected using a combination of contact definitions, 1D structural elements, and, where necessary, node merging. The entire ARL torso model has a mass of 30.7 kg and contains 271 individually meshed components joined by beam elements. A number of different material models were adopted in order to analyse material characterisations and parameters, then the model was validated in frontal impact at a velocity of 6.7056 m/s (Impactor dimensions:  $d = 152.4$  mm and  $L = 152.4$  mm). However, it is important to acknowledge certain limitations of the ARL torso FE model. While the model offers valuable insights into ballistic impact mechanisms, it may not accurately represent a broad range of thoracic and abdominal trauma scenarios as the model has only been validated for one impact velocity. Consequently, the model needs further

validation and refinement in order to enhance its applicability to real-world military scenarios, including BABT. Additionally, its computational complexity and substantial resource requirements should be considered when choosing it for specific applications. While the model was dedicated for the LS-DYNA software, it can be used on other FE platforms such as ParaDyn, Sierra, and ALE3D.

**Human torso model summary.** As demonstrated in Table 4, it is apparent that the majority of human torso FE models have been developed using civilian anthropometric data (Roberts, O'Connor, and Ward 2005; Shen et al. 2008; Roth et al. 2013; Tang et al. 2019), with only a few based on military anthropometry (Ng and Niu 2018; Hampton and Kleinberger 2018b; Zochowski 2019). Furthermore, most models are based on 50<sup>th</sup> percentile (civilian or military) males, despite the fact that females differ to males, particularly in the thorax and abdominal body regions, not only in size, but also anthropometry and anatomy, with different organ positions and tissue mechanical properties (e.g. Burrowes et al. 2023). Consequently, females have a lower tolerance to injury than males, and a higher chance of sustaining severe injuries (Kimpara et al. 2005). Hence, current torso models do not address sex-specific differences in body armour performance and injury response, which are important considerations when applying them to female populations. Nevertheless, this highlights the need to develop new models for other individuals, or alternatively, create a straightforward scaling technique to adapt these models for females as well as subjects of different sizes.

A further challenge lies with material model development, as there are few known material properties for high strain rates, consequently, material models at somewhat lower (i.e. automotive) strain rates have often been used to analyse BFD scenarios. Furthermore, the current FE models used for simulating thoracic injuries, including rib fractures, often lack an accurate representation of the contribution of intercostal muscles due to limited knowledge about the mechanical behaviour and fibre orientations of these muscles (Hamzah et al. 2013). Moreover, while there are both cadaveric and real-world data on armour BFD, for example, Weisenbach et al. (2018) and Bir (2015), this data is quite limited, and the majority of cadaveric tests or real-world impact data available for validation purposes pertain to automotive blunt impact scenarios for frontal, side and rear-impact crash events. Finally, to the best of the

authors' knowledge, except HUBYX model, which is available within Altair Hyperwork library, all other torso models discussed here are not commercially available.

One critical aspect deserving special attention is the integration of trauma registries into the research framework. By combining trauma registry data with radiological, clinical, and simulation-based findings, researchers can gain a more comprehensive understanding of the effects of BFD on the human body and the resulting implications for body armour development. Trauma registries provide real-world validation for FE models, improving model biofidelity by offering insights into injury severities, patterns of injury, and the overall distribution of trauma in the human torso; thus, they are a critical factor in body armour design. Moreover, trauma registries include diverse populations, thereby making them highly relevant in guiding body armour development for different military users. Combining real-world registry data with FE models can consequently provide unique insights into injury mechanisms, contributing towards the advancement of emerging body armour materials and torso plate design (Bir et al. 2017).

In the current systematic review, the PRISMA methodology and guidelines were strictly adhered to when searching for relevant publications on the use of FE models for BFD and body armour design, and as far as possible, the papers were reviewed in a critical unbiased manner. Nevertheless, the study was not without limitations. For example, only publications in English were included in the current analysis, and it is possible that there are relevant papers on this topic published in other languages which may have contributed further insights into FE analysis of body armour BFD. Furthermore, only papers published from 1980 were reviewed; however, this was not considered to be a significant drawback as prior to this time, significant limitations in computational power rendered FE analysis to basic models representing physical phenomena. Additionally, unlike other disciplines such as civil engineering, prior to 1980, FE models and techniques in the newly emerging field of biomechanics, and more specifically impact biomechanics, were not particularly advanced.

#### 4. Conclusions

A systematic review of the openly accessible literature was conducted using the Preferred Reporting Items for Systematic Reviews and Meta-Analyses method to investigate the use of the FE method as tool for

predicting injury from armour BFD. In summary, the main conclusions are as follows:

- The review highlights the diversity of modelling approaches employed for studying BFD and BABT. In addition to FE analysis, other widely used techniques, such as clay-based models and gelatine models, have been instrumental in advancing the current understanding of BFD mechanisms.
- Clay-based models, with their ability to simulate transient deformation behaviour, have provided valuable insights into the response of body armour materials to impact. Gelatine models, which replicate the human torso's soft tissue characteristics, offer a practical means of evaluating potential injury risks.
- Clay and gelatine models have specific uses and implications for body armour development. Clay models are valuable for assessing material behaviour and can be an important tool for optimising armour materials for enhanced protection. Gelatine models, owing to their biofidelity, are critical for evaluating injury potential and assessing body armour performance.
- Over the last few decades, although there has been a growing interest in BABT, only a few FE models have been exclusively developed for ballistic impacts and BFD.
- Further studies should involve refining and expanding these modelling techniques. This includes developing more comprehensive material property databases, refining anthropometric models to represent diverse populations, and exploring emerging technologies for more accurate model predictions.
- One potential method to aid in validating torso FE models would be to correlate trauma registry data from combatants sustaining BABT, including both radiologic and clinical findings, with predictions from FE models.
- Future research should also focus on developing human torso FE models based on female anatomies to address sex-specific differences in body armour performance and injury response. Additionally, FE models representing both males and females of different sizes are needed in order to capture anthropometrical variations in both the military and civilian populations.
- The findings from these models have significant implications for injury mitigation and protection, guiding the development of more effective and safer body armour solutions for both military and civilian applications.

- Acknowledging the limitations in the current state of research, this review highlights areas for improvement. Researchers should focus on continuing to address challenges, such as the need for more accurate material properties for model development.

## Acknowledgments

The authors express their appreciation to the Defence Science and Technology Group (DSTG) for funding this work (Contract No: 10437).

## Disclosure statement

No potential conflict of interest was reported by the authors.

## References

- Backaitis SH. 1994. Biomechanics of impact injury and injury tolerances of the thorax-shoulder complex. Society of Automotive Engineers.
- Bass CR, Salzar RS, Lucas SR, Davis M, Donnellan L, Folk B, Sanderson E, Waclawik S. 2006. Injury risk in behind armor blunt thoracic trauma. *Int J Occup Saf Ergon*. 12(4):429–442. doi:10.1080/10803548.2006.11076702.
- Batra RC, Pydah A. 2020. Impact analysis of PEEK/ceramic/gelatin composite for finding behind the armor trauma. *Compos Struct*. 237:111863. doi:10.1016/j.compstruct.2020.111863.
- Bir C. 2000. The evaluation of blunt ballistic impacts of the thorax. Detroit, MI: Wayne State University.
- Bir C. 2015. Ballistic injury biomechanics. In *Accidental Injury: biomechanics and prevention*. New York, NY: Springer New York. p. 829–839.
- Bir C, Lance R, Stojisih-Sherman S, Cavanaugh J. 2017. Behind armor blunt trauma: recreation of field cases for the assessment of backface signature testing. Paper presented at Proceedings of the 30th International Symposium on Ballistics. doi:10.12783/ballistics2017/16912.
- Bir C, Viano D, King A. 2004. Development of biomechanical response corridors of the thorax to blunt ballistic impacts. *J Biomech*. 37(1):73–79. doi:10.1016/s0021-9290(03)00238-0.
- Bodo M, Bracq A, Delille R, Marechal C, Roth S. 2017. Thorax injury criteria assessment through non-lethal impact using an enhanced biomechanical model. *J Mech Med Biol*. 17(07):1740027. doi:10.1142/S0219519417400279.
- Bouamoul A, Lévesque H. 2007. Development and validation of a finite element human torso model under blunt ballistic impact.
- Bracq A. 2021. Numerical recreation of police field cases on a human body FE model: first insights into BABT. *Skin*. 1:1.
- Bracq A, Bourel B, Delille R, Maréchal C, Haugou G, Lauro F, Roth S, Mauzac O, Bir C. 2020. Numerical recreation of police field cases on a human body FE model: first

- insights into BABT. Personal Armour Systems Symposium.
- Bracq A, Delille R, Benjamin B, Maréchal C, Haugou G, Lauro F, Roth S, Mauzac O. 2018a. Behind armour blunt trauma assessment by means of experimental and numerical approaches. Proceedings of the Personal Armour Systems Symposium.
- Bracq A, Delille R, Benjamin B, Maréchal C, Haugou G, Lauro F, Roth S, Mauzac O. 2018b. Risk of rib fractures assessment during kinetic energy projectile impact through experiments and modelling on a human torso FE model. Proceedings of the Personal Armour Systems Symposium; Washington DC: Federal Business Council.
- Bracq A, Delille R, Bourel B, Maréchal C, Haugou G, Lauro F, Roth S, Mauzac O. 2019. Numerical recreation of field cases on a biofidelic human FE model involving deformable less-lethal projectiles. *Hum Factors Mech Eng Def Saf.* 3(1):5. 2019/07/31doi:10.1007/s41314-019-0022-8.
- Bracq A, Haugou G, Bourel B, Delille R, Maréchal C, Lauro F, Roth S, Mauzac O. 2018. Characterization of a visco-hyperelastic synthetic gel for ballistic impacts assessment. In: *Dynamic behavior of materials, Vol. 1.* Bethel, CT: Springer. p. 109–113.
- Bracq A, Marechal C, Delille R, Bourel B, Roth S, Mauzac O. 2017. Methodology for ballistic blunt trauma assessment. *Comput Methods Biomech Biomed Engin.* Oct20: 31–32.
- Breeze J, Newbery T, Pope D, Midwinter MJ. 2014. The challenges in developing a finite element injury model of the neck to predict the penetration of explosively propelled projectiles. *J R Army Med Corps.* 160(3):220–225. Epub 20130910. doi:10.1136/jramc-2013-000109.
- Burrowes KS, Ruppige M, Lowry A, Zhao D. 2023. Sex matters: the frequently overlooked importance of considering sex in computational models. *Front Physiol.* 14:1186646. Epub 20230713. doi:10.3389/fphys.2023.1186646.
- Bustamante MC, Barker J, Rafaels KA, Bir C, Singh D, Sathananthan P, Cronin DS. 2019. Shell plate method of reconstructing behind armour blunt trauma impact scenarios for soft armour using a detailed thorax model. Paper presented at Proceedings of the Conference proceedings International Research Council on the Biomechanics of Injury, IRCOBI.
- Campbell BM, Cronin DS. 2014. Coupled human body and side impact model to predict thoracic response. *Int J Crashworthiness.* 19(4):394–413. doi:10.1080/13588265.2014.909561.
- Cannon L. 2001. Behind armour blunt trauma-an emerging problem. *J R Army Med Corps.* 147(1):87–96. doi:10.1136/jramc-147-01-09.
- Carr DJ, Horsfall I, Malbon C. 2016. Is behind armour blunt trauma a real threat to users of body armour? A systematic review. *J R Army Med Corps.* 162(1):8–11. Epub 20131113. doi:10.1136/jramc-2013-000161.
- Cavanaugh JM, Nyquist GW, Goldberg SJ, King AI. 1986. Lower abdominal tolerance and response. *SAE Trans.* :611–633.
- Chan H. 2021. Investigation of the torso armour backface deformation ballistic standard. The Australian National University.
- Chang F. 2001. The development and validation of a finite element human thorax model for automotive impact injury studies. Paper presented at Proceedings of the ASME International Mechanical Engineering Congress and Exposition; American Society of Mechanical Engineers. doi:10.1115/IMECE2001/AMD-25445.
- Choudhury S, Yerramalli CS, Guha A, Ingle S. 2022. Prediction and mitigation of behind armor blunt trauma in composite plate armor using rubber backing or air gaps. *Eur J Mechan A Solids.* 93:104533. doi:10.1016/j.euromechsol.2022.104533.
- Chung J, Cavanaugh JM, King AI, Koh S-W, Deng Y-C. 1999. Thoracic injury mechanisms and biomechanical responses in lateral velocity pulse impacts.
- Cronin DS. 2006. Wave and deformation effects in behind armour blunt trauma. *J Biomech.* 39:S163. doi:10.1016/S0021-9290(06)83562-1.
- Cronin DS. 2012. Application of a detailed thorax model to investigate behind armour blunt trauma. Paper presented at Proceedings of the IRCOBI Conference Proceedings.
- Cronin DS. 2015. Investigation of lung response resulting from behind armour blunt trauma impact scenarios. Paper presented at Proceedings of the International Research Council on Biomechanics of Injury (IRCOBI). p. 722–723.
- Cronin DS, Bustamante MC, Barker J, Singh D, Rafaels KA, Bir C. 2021. Assessment of thorax finite element model response for behind armor blunt trauma impact loading using an epidemiological database. *J Biomech Eng.* 143(3):031007.
- Cronin DS, Rafaels K, Bir C, Barker J, Singh D, Bustamante M, Sathananthan P. 2018. Reconstruction of behind armour blunt trauma impact scenarios for soft armour using a detailed thorax model. Paper presented at Proceedings of the International Research Council on Biomechanics of Injury (IRCOBI). p. 752–753.
- Cronin DS, Worswick M, Ennis A, Bourget D, Williams K, Pageau G. 2001. Behind armour blunt trauma for ballistic impacts on rigid body armour. Paper presented at Proceedings of the 19th International Symposium on Ballistics Interlaken, Switzerland.
- Dominiak J, Stempień Z. 2012. Finite-element-based modeling of ballistic impact on a human torso protected by textile body armor. *Innovative materials & technologies in made-up textile articles, protective clothing and footwear.*
- Eaton MAK, McMahon JA, Salzar RS. 2022. Evaluating the limits in the biomechanics of blunt lung injury. *J Biomech Eng.* 144:090801.
- Gad A, Gao X-L. 2020. Modeling of deformations of Roma Plastilina# 1 clay in column-drop tests by incorporating the coupled strain rate and temperature effects. *Mech Adv Mater Struct.* 27(13):1154–1166. doi:10.1080/15376494.2020.1712629.
- Gilson L, Rabet L, Imad A, Coghe F. 2020. Experimental and numerical assessment of non-penetrating impacts on a composite protection and ballistic gelatine. *Int J Impact Eng.* 136:103417. doi:10.1016/j.ijimpeng.2019.103417.
- Gilson L, Rabet L, Imad A, Nsiampa N, Coghe F. 2021. Ballistic impact response of a fluid/structure coupling-based modification of human thorax modelling. *J Mech Behav Biomed Mater.* 119:104493. Epub 20210327. doi:10.1016/j.jmbbm.2021.104493.

- Graham MJ, Zhang TG. 2019. Finite element analysis of geometric effects on ballistic clay backing material.
- Hampton CE, Kleinberger M. 2018a. Computational human torso model validation for frontal blunt trauma. Paper presented at Proceedings of the ASME International Mechanical Engineering Congress and Exposition; American Society of Mechanical Engineers. doi:10.1115/IMECE2018-88382.
- Hampton CE, Kleinberger M. 2018b. Material models for the human torso finite element model.
- Hamzah M, Subit D, Boruah S, Forman J, Crandall J, Ito D, Ejima S, Kamiji K, Yasuki T. 2013. An inverse finite element approach for estimating the fiber orientations in intercostal muscles. Paper presented at Proceedings of the IRCOBI Conference;
- Hernandez C, Buchely MF, Maranon A. 2015. Dynamic characterization of Roma Plastilina No. 1 from Drop Test and inverse analysis. *Int J Mech Sci.* 100:158–168. doi:10.1016/j.ijmecsci.2015.06.009.
- Hernandez C, Maranon A, Ashcroft I, Casas-Rodriguez J. 2012. Inverse methods for the mechanical characterization of materials at high strain rates. Paper presented at Proceedings of the EPJ Web of Conferences; EDP Sciences. doi:10.1051/epjconf/20122604022.
- Kim Y, Kim YA, Park SH, Kim Y. 2022a. Hybrid numerical modeling of ballistic clay under low-speed impact using artificial neural networks. arXiv preprint arXiv: 220514893.
- Kim YA, Kim Y, Park SH, Kim Y. 2022b. Empirical and numerical study on Roma Plastilina #1 ballistic clay under various drop impact tests. *Mech Adv Mater Struct.* 30(18):3699–3709. doi:10.1080/15376494.2022.2081747.
- Kimpara H, Lee JB, Yang KH, King AI, Iwamoto M, Watanabe I, Miki K. 2005. Development of a three-dimensional finite element chest model for the 5th percentile female. *Stapp Car Crash J.* 49:251–269. doi:10.4271/2005-22-0012.
- Kroell CK, Schneider DC, Nahum AM. 1971. Impact tolerance and response of the human thorax.
- Lewis EA. 2005. Pencilling: a novel behind armour blunt trauma injury. Cranfield University.
- Liberati A, Altman DG, Tetzlaff J, Mulrow C, Gotzsche PC, Ioannidis JP, Clarke M, Devereaux PJ, Kleijnen J, Moher D. 2009. The PRISMA statement for reporting systematic reviews and meta-analyses of studies that evaluate healthcare interventions: explanation and elaboration. *BMJ.* 339(jul21 1):b2700–b2700. 21Epub 20090721. doi:10.1136/bmj.b2700.
- Liden E, Berlin R, Janzon B, Schantz B, Seeman T. 1988. Some observations relating to behind-body armour blunt trauma effects caused by ballistic impact. *J Trauma.* 28(1 Suppl):S145–S148. doi:10.1097/00005373-198801001-00029.
- Lim CT, Shim VPW, Ng YH. 2003. Finite-element modeling of the ballistic impact of fabric armor. *Int J Impact Eng.* 28(1):13–31. doi:10.1016/S0734-743X(02)00031-3.
- Mauzac O, Paquier C, Barbillon F, Mabire P, Jacquet J, Debord E, Riesemann A. 2012. Comparative assessment of Behind Armour Blunt Trauma (BABT) by means of a novel transparent synthetic gel. Paper presented at Proceedings of the Personal Armour Systems Symposium;
- Merkle AC, Ward EE, O'Connor JV, Roberts JC. 2008. Assessing behind armor blunt trauma (BABT) under NIJ standard-0101.04 conditions using human torso models. *J Trauma.* 64(6):1555–1561. doi:10.1097/TA.0b013e318160ff3a.
- MurthyThota N, Eepaarachchi JA, Lau K. 2012. Develop and validate a biomechanical surrogate of the human thorax using corrugated sheets: a feasibility study. Paper presented at Proceedings: the 7th Australasian Congress on Applied Mechanics (ACAM 7), 9–12 December 2012, the University of Adelaide, North Terrace Campus/ National Committee on Applied Mechanics of Engineers Australia: the 7th Australasian Congress on Applied Mechanics (ACAM 7), 9–12 December 2012, University of Adelaide, North Terrace Campus/National Committee on Applied Mechanics of Engineers Australia; Engineers Australia Barton ACT.
- Ndompetelo N. 2016. Numerical assessment of non-lethal projectile thoracic impacts.
- Ng L, Niu E. 2018. Verification and validation report for ATBM torso finite element model.
- Nguyen LH, Lässig TR, Ryan S, Riedel W, Mouritz AP, Orifici AC. 2016. A methodology for hydrocode analysis of ultra-high molecular weight polyethylene composite under ballistic impact. *Compos A Appl Sci Manuf.* 84: 224–235. doi:10.1016/j.compositesa.2016.01.014.
- Niu Y, Shen W, Stuhmiller JH. 2007. Finite element models of rib as an inhomogeneous beam structure under high-speed impacts. *Med Eng Phys.* 29(7):788–798. Epub 20061011. doi:10.1016/j.medengphy.2006.08.015.
- Page MJ, McKenzie JE, Bossuyt PM, Boutron I, Hoffmann TC, Mulrow CD, Shamseer L, Tetzlaff JM, Akl EA, Brennan SE, et al. 2021. The PRISMA 2020 statement: an updated guideline for reporting systematic reviews. *BMJ.* 372:71. Epub 20210329. doi:10.1136/bmj.n71.
- Rahbek DB. 2015. Finite element simulations of drop indentations into oily clay.
- Rahman M. 2013. Impact resistance of laminated hybrid composite panels composed of compliant and rigid plies. Canberra: University of New South Wales.
- Roberts JC, Merkle AC, Biermann PJ, Ward EE, Carkhuff BG, Cain RP, O'Connor JV. 2007. Computational and experimental models of the human torso for non-penetrating ballistic impact. *J Biomech.* 40(1)2018-10-0:125–136. 6Epub 20051222. doi:10.1016/j.jbiomech.2005.11.003.
- Roberts JC, O'Connor JV, Ward EE. 2005. Modeling the effect of nonpenetrating ballistic impact as a means of detecting behind-armor blunt trauma. *J Trauma.* 58(6): 1241–1251. doi:10.1097/01.ta.0000169805.81214.dc.
- Rocksén D, Arborelius UP, Gustavsson J, Gunther M. 2020. Severe, transient pulmonary ventilation-perfusion mismatch in the lung after porcine high velocity projectile behind armor blunt trauma. *Exp Lung Res.* 46(8):271–282. Epub 20200722. doi:10.1080/01902148.2020.1797246.
- Roth S, Torres F, Feuerstein P, Thorax-Pierre K. 2013. Anthropometric dependence of the response of a thorax FE model under high speed loading: validation and real world accident replication. *Comput Methods Programs Biomed.* 110(2):160–170. MayEpub 20121211. doi:10.1016/j.cmpb.2012.11.004.
- Roth S. 2020. Three-dimensional numerical study of the influence of the thorax positioning submitted to blast loading: consequences on body trauma. *Mech Adv Mater Struct.* 27(5):396–402. 2doi:10.1080/15376494.2018.1474304.

- Scherer RW, Saldanha IJ. 2019. How should systematic reviewers handle conference abstracts? A view from the trenches. *Syst Rev*. 8(1):264. doi:10.1186/s13643-019-1188-0.
- Seng F, Hackney D, Goode T, Noever A, Hammond A, Velasco I, Peters K, Pankow M, Schultz S. 2021. Dynamic back face deformation measurement with a single optical fibre. *Int J Impact Eng*. 150:103800. doi:10.1016/j.ijimpeng.2020.103800.
- Shedge R, Krishan K, Warriar V, Kanchan T. 2023. Postmortem changes. In *StatPearls*. Treasure Island, FL: StatPearls Publishing LLC.
- Shen J, Taddei L, Roth S. 2022. Numerical modeling of a human tissue surrogate SEBS gel under high velocity impacts: investigation of the effect of the strain rate in an elasto-hydrodynamic law. *Mech Adv Mater Struct*. 29(2):241–249. doi:10.1080/15376494.2020.1761490.
- Shen W, Niu Y, Bykanova L, Laurence P, Link N. 2010. Characterizing the interaction among bullet, body armor, and human and surrogate targets. *J Biomech Eng*. 132(12):121001. doi:10.1115/1.4002699.
- Shen W, Niu Y, Mattrey RF, Fournier A, Corbeil J, Kono Y, Stuhmiller JH. 2008. Development and validation of subject-specific finite element models for blunt trauma study. *J Biomech Eng*. 130(2):021022. doi:10.1115/1.2898723.
- Talmy T, Itah A, Ahimor A, Drukarov D, Shovali A, Malkin M, Shina A, Gendler S, Tsur AM, Almog O. 2023. Close-range fire inflicting behind armor blunt trauma: case-series and implications for battlefield care. *Mil Med*. Epub 20230830. doi:10.1093/milmed/usad340.
- Tam W, Dorn M, Gotts P. 2000. A new method for quantifying behind armour blunt trauma. Paper presented at Proceedings of the Personal Armour Systems Symposium.
- Tang F, Guo Z, Yuan M, Qian X, Du Z. 2019. Numerical simulation for behind armor blunt trauma of human torso under non-penetrating ballistic impact. *bioRxiv*.586594.
- Thota N, Epaarachchi J, Lau KT. 2014a. Viscous criterion and its relation with the projectile-thorax energy interactions.
- Thota NM, Epaarachchi JA, Lau KT. 2014b. Development and validation of a thorax surrogate FE model for assessment of trauma due to high speed blunt impacts. *JBSE*. 9(1):JBSE0008–JBSE0008. doi:10.1299/jbse.2014jbse0008.
- Viano DC, Lau IV, Asbury C, King AI, Begeman P. 1989. Biomechanics of the human chest, abdomen, and pelvis in lateral impact. *Accid Anal Prev*. 21(6):553–574. doi:10.1016/0001-4575(89)90070-5.
- Weisenbach CA, Logsdon K, Salzar RS, Chancey VC, Brozoski F. 2018. Preliminary investigation of skull fracture patterns using an impactor representative of helmet back-face deformation. *Mil Med*. 183(suppl\_1):287–293. doi:10.1093/milmed/usx210.
- Wen Y, Xu C, Wang S, Batra RC. 2015. Analysis of behind the armor ballistic trauma. *J Mech Behav Biomed Mater*. 45:11–21. Epub 20150121. doi:10.1016/j.jmbbm.2015.01.010.
- Wen YK, Xu C, Wang HS, Chen AJ, Batra RC. 2013. Impact of steel spheres on ballistic gelatin at moderate velocities. *Int J Impact Eng*. 62:142–151. doi:10.1016/j.ijimpeng.2013.07.002.
- Ye S, Xu Y, Zhou Y, Cheng J, Huang JY, Cai Y, Yao X, Luo S. 2022. Penetration dynamics of steel spheres into a ballistic gelatin: experiments, nondimensional analysis, and finite element modeling. *Int J Impact Eng*. 162:104144. doi:10.1016/j.ijimpeng.2021.104144.
- Zhang TG, Ivancik J, Mrozek RA, Satapathy SS. 2017. Material characterization of ballistic Roma Plastilina No. 1 Clay. Paper presented at Proceedings of the 30th International Symposium on Ballistics. doi:10.12783/ballistics2017/17041.
- Zochowski P. 2019. Numerical methods for the analysis of behind armor ballistic trauma.